2009

The Type VI Secretion System of Burkholderia cenocepacia: a study of actin cytoskeleton remodeling and involvement in host cell death

Daniel W. Hynes
Western University

The Type VI Secretion System of *Burkholderia cenocepacia:* a study of actin cytoskeleton remodeling and involvement in host cell death

(Spine title: The T6SS of *Burkholderia cenocepacia*)

(Thesis format: Monograph)

by

Daniel W. Hynes

Graduate Program
in
Microbiology & Immunology

A thesis submitted in partial fulfilment
of the requirements for the degree of
Master of Science

School of Graduate and Postdoctoral Studies
The University of Western Ontario
London, Ontario, Canada
August, 2009

Abstract

Burkholderia cenocepacia is an opportunistic pathogen of cystic fibrosis patients. *B. cenocepacia* encodes a type VI secretion system (T6SS) under control by the global negative regulator, AtsR. This study demonstrates that while the T6SS is not involved in the characteristic phagosome maturation delay associated with *B. cenocepacia*, it may play a role in the induction of host cell death. The formation of actin-rich protrusions within infected host cells, previously shown as dependent upon T6SS function, is not a prelude to this cell death, as a mutant deficient in the induction of actin rearrangement still induced cell death. Furthermore, other unknown virulence factors regulated by AtsR may contribute to host cell death, as only loss of T6SS function in conjunction with loss of normal global regulation resulted in reduced host cell death. The host cell death studied appears to not proceed through caspase-3 dependent pathways.

Key words
Burkholderia cenocepacia, cell death, apoptosis, type VI secretion system

Dedication

To Patricia.

Acknowledgements

I would like to thank my supervisor, Dr. Miguel Valvano, for inviting me to contribute to his lab. I would also like to thank members of my advisory committee, Dr. Sung Kim and Dr. John McCormick, for their support and guidance. Also, thank you to members of the Valvano Lab, past and present, who have contributed to a fun and dynamic learning environment. A special thank you to Dr. Daniel Aubert, whose hard work produced the foundation for my project as well as numerous others. A thank you to my family for helping me along the way during my studies. I would like to thank Nana for her instrumental contribution to the writing process. Last and certainly not least, I would like to thank Patricia Goodman for her tireless efforts to support me throughout my graduate studies.

Contents

List of Figures

List of Tables

List of Abbreviations

AAA+	ATPase associated with a variety of cellular activities
ADP	Adenosine diphosphate
APAF	Apoptotic peptidase activating factor
ATP	Adenosine triphosphate
Bak	Bcl-2 homologous antaganoist/killer
Bax	Bcl-2 associated X
Bcl-2	B-cell CLL/lymphoma 2
Bcc	*Burkholderia cepacia* complex
BcCV	*Burkholderia cenocepacia*-containing vacuole
caspase	Cysteine-aspartic acid protease
CF	Cystic fibrosis
CFTR	Cystic fibrosis transductance regulator
clp	Caseinolytic peptidase
Cm	Chloramphenicol
DMEM	Dulbecco's Modified Eagle Medium
FBS	Fetal Bovine Serum
FOV	Field of view
FHA	Fork head association
G+C	Guanine + cytosine
kDa	kilodalton
LAMP-1	Lysosome-associated membrane protein 1
LB	Luria-Bertani
Mb	Megabase
mM	millimolar
MCS	Multiple cloning site
Mob	Mobilization element
MOI	Multiplicity of infection
nm	nanometer
ori	Origin of replication
PBS	Phosphate-buffered saline
Rip-1	Ras-interacting protein 1
rDNA	Ribosomal deoxyribonucleic acid
RFP	Ref fluorescent protein
ROS	Reactive oxygen species
Tet	Tetracycline
Tp	Trimethoprim
v/v	volume per volume
w/v	weight per volume

Chapter 1

Introduction

1.1 - *Burkholderia cepacia* complex bacteria

The genus *Burkholderia* comprises Gram-negative bacilli that can be found ubiquitously in the environment (Mahenthiralingam *et al.,* 2005). The taxonomy of the genus was convoluted, as its members were initially identified as belonging to the genus *Pseudomonas* (Ballard *et al.,* 1970; Burkholder, 1950). Once appropriately identified, the new genus *Burkholderia* contained 7 species, one of which, *B. cepacia,* was subdivided into genomovars consisting of bacteria that had similar phenotypes, but distinct genotypes (Vandamme *et al.,* 1997). This cluster of genomovars was referred to as the *Burkholderia cepacia* complex (Bcc). These genomovars have since been assigned species names, and the Bcc have grown to include at least 17 distinct species (Mahenthiralingam *et al.,* 2008).

The original expansion in species number and distinctiveness can be attributed to the effective use of polyphasic taxonomic methods (Vandamme *et al.,* 1996). These methods rely on genotypic information such as G+C content of the genome, restriction patterns using restriction fragment length polymorphisms, genome size, ribotyping, and phage typing. Phenotypic information obtained includes chemotaxonomic markers such as the presence of mycolic acids, polar lipids, or isoprenoid quinones, as well as features such as morphology, or enzymology of particular bacteria being analyzed (Vandamme *et al.,* 1996). In particular, the original species of the Bcc were identified based on sharing a high degree of 16S rDNA and *recA* sequence similarity, with lower levels of DNA-DNA hybridization (Vandamme *et al.,* 1997; 2000; 2002; 2003; Coenye and Vandamme, 2003). More recently, taxonomic methods like multilocus sequence typing (MLST) (Spilker *et al.,*

2009; Mahenthiralingam *et al.,* 2006) contributed to expand the documented diversity of the Bcc. Table 1 lists the current members of the Bcc.

1.2 - Possible industrial applications and their principal barrier

Bcc members could be pathogenic for plants. Indeed, the first reported isolate of *Burkholderia* was discovered as the causative agent of soft onion rot (Burkholder, 1950). Bcc members also exist as endosymbionts, which protect plants from infection, through the production of antimicrobial compounds (Bevivino *et al.,* 1998), and promote plant growth through the secretion of plant growth factors (Estrada-De Los Santos *et al.,* 2001). Bcc bacteria can degrade a wide range of man-made pollutants, with some species capable of degrading aromatic substrates common to herbicides and pesticides (Mars *et al.,* 1996). Some of these characteristics suggest the Bcc would be suitable for biocontrol and bioremediation (Mars *et al.,* 1996). However, the metabolic diversity of Bcc members also contributes to extremely high levels of resistance to antimicrobials displayed by these bacteria. Thus, Bcc members are successful opportunistic pathogens in certain human populations, mainly in individuals who are therapeutically immunosuppressed (for instance, following organ transplantation), or those suffering from chronic granulomatous disease (Bottone *et al.,* 1975) and cystic fibrosis (Speert *et al.,* 2002).

Table 1: Current Bcc biodiversity within the Cardiff collection (adapted from Mahenthiralingam *et al.* 2008). Statistics obtained from Cardiff, UK regarding the increasing number of Bcc bacterial species as phylogenetic analysis technology has advanced. Cystic fibrosis clinical samples, non-CF clinical samples, and samples obtained from the environment are compared. The Cardiff collection is used as an example of a phylogenetic analysis containing 20 different classifications of species or groups within the *Burkholderia cepacia* complex, demonstrating the increasing phylogenetic diversity of the Bcc.

CF: cystic fibrosis clinical sample; Clinical: isolates found in non-CF clinical samples; Env.: isolates obtained from environmental samples.

Species or MLST subgroup	Genomovar	Total No.	CF (%)	Clinical (%)	Enviro. (%)
B. cepacia	I	45	14 (31)	12 (27)	17 (38)
B. multivorans	II	93	77 (83)	9 (10)	6 (6)
B. cenocepacia IIIA	III	148	123 (83)	21 (14)	2 (1)
B. cenocepacia IIIB	III	123	84 (68)	6 (5)	25 (20)
B. cenocepacia IIIC	III	16	0	0	16 (100)
B. cenocepacia IIID	III	14	14 (100)	0	0
B. stabilis	IV	25	9 (36)	9 (36)	3 (12)
B. vietnamiensis	V	41	16 (39)	5 (12)	17 (41)
B. dolosa	VI	7	6 (85)	0	1 (14)
B. ambrifaria	VII	113	6 (5)	0	106 (94)
B. anthina	VIII	10	2 (20)	0	8 (80)
B. pyrrocinia	IX	17	1 (6)	0	16 (94)
B. ubonensis	X	2	0	1 (50)	1 (50)
Group K	-	59	20 (34)	5 (8)	10 (17)
BCC1	-	4	4 (100)	0	0
BCC2	-	8	4 (50)	1 (12)	3 (37)
BCC3	-	13	4 (31)	2 (15)	1 (7)
BCC4	-	3	1 (33)	0	2 (67)
BCC5	-	18	1 (5)	1 (5)	16 (89)
BCC6	-	39	2 (5)	0	37 (95)
	Total	798	388	72	287

1.3 - Chronic Granulomatous Disease

Chronic granulomatous disease (CGD) is caused by mutations in genes encoding subunits of the nicotinamide adenine dinucleotide phosphate oxidase (NADPH) complex (Heyworth *et al.,* 2003). Under normal circumstances, the NADPH oxidase complex is assembled on the membrane of maturing phagosomes after phagocytosis (Minakami and Sumimotoa, 2006). Once the complex is assembled, the enzyme becomes functional and can produce an oxidative burst, whereby the phagosomal lumen is flooded with volatile reactive oxygen species (ROS) (Minakami and Sumimotoa, 2006). Mutations causing CGD abrogate normal NADPH oxidase assembly and, therefore, result in negligible production of ROS within the phagosome. As a consequence, CGD patients develop opportunistic bacterial and fungal infections since their neutrophils and macrophages are unable to produce reactive oxygen species, a critical component of the innate immune system. In addition, insufficient NADPH-oxidase mediated ROS production causes granulomas to form within large organs as a result of recurrent infections (Holland, 2009).

1.4 - Cystic Fibrosis

Cystic fibrosis (CF) is an autosomal recessive disorder that affects approximately 1 in 3600 people (Dupuis *et al.,* 2005). It is the most common lethal inherited disorder amongst the Caucasian population, but is also known to be a prevalent disorder amongst certain ethnic groups, including Ashkenazi Jews (Abeliovich *et al.,* 1992). Despite its prevalence amongst certain ethnic groups, its

incidence is not constrained by race and cases have been reported throughout the world, regardless of ethnicity (Lakeman *et al.*, 2008).

The disease results from mutations in the gene encoding a membrane protein that functions as a chloride ion transductance regulator called the Cystic Fibrosis Transductance Regulator (CFTR). Currently, there are over 1600 different *cftr* mutations that can cause CF (http://www.genet.sickkids.on.ca/cftr/Home.html) and which result in various classes of CFTR functional defects: (i) class I mutations cause defective protein synthesis, (ii) class II mutations cause abnormal protein processing and trafficking, (iii) class III mutations cause dysregulation of CFTR gating, (iv) class IV mutations cause reduced conductance and (v) class V mutations cause reduced biosynthesis of fully active CFTR (Zielenski, 2000). The most prevalent mutation is the ΔF508 mutation, with 70% of all CF patients being homozygous for this mutation. A 3-bp deletion in exon 10 causes a loss of a phenylalanine at position 508 of the gene product (Zielenski, 2000). Loss of F508 results in the incorrect trafficking of the CFTR gene product to the cell membrane. Thus, the CFTR protein is degraded within the endoplasmic reticulum and negligible amounts of the protein reach the cell membrane. (Cheng *et al.*, 1990).

CFTR defects cause incorrect transductance of chloride ions across the cell membrane, which in turn results in dehydrated mucous in the lumen of various organs. This viscous, dehydrated mucous affects the diffusion of enzymes in the digestive system and mucocilliary clearance in the lungs. Symptoms affecting the digestive system were the root cause of low life expectancy rates in CF patients in

the previous century, as most people with the disease did not survive beyond ten years of age (Lakeman *et al.,* 2008).

With the advent of orally administered digestive enzymes, the life span of patients increased dramatically, and respiratory symptoms began to increase in significance from a medical perspective. Without proper mucocilliary clearance, inhaled bacteria are caught in the airways, resulting in chronic pulmonary inflammation (O'Sullivan and Freedman, 2009). CF lung disease causes the highest rates of morbidity and mortality within the CF patient population (Zielenski, 2000). CF patients routinely become chronically infected with bacteria that normally only affect the severely immunosuppressed, as well as a myriad of bacterial pathogens that are acutely adapted to survive and thrive in the growth conditions provided by the altered physiology in the CF lungs.

Every single species of the Bcc has been isolated from the sputum of CF patients (Coenye and Vandamme, 2003), but approximately 83% of all Bcc-positive lung infections in CF patients in Canada include *B. cenocepacia* (Speert *et al.,* 2002). Similar numbers of infections manifest either without symptoms or with a rapid decline in pulmonary function due to chronic infection. In rare cases, Bcc-positive CF patients succumb to '*Cepacia* Syndrome', an acute disease characterized by septicemia, necrotizing pneumonia, and mortality (Mahenthiralingam *et al.,* 2005). As with other members of the Bcc, treatment scenarios are complicated due to extremely high resistance to all but a few antibiotics. These bacteria also express numerous virulence factors, such as cable pili, flagella, surface exopolysaccharide, catalase and superoxide dismutase, and others (Valvano *et al.,* 2005). *B. cenocepacia*

can evade host innate immunity, as it delays the maturation of the phagosome through an unknown mechanism (Lamothe *et al.,* 2007). Furthermore, *B. cenocepacia* can exploit CFTR deficient macrophages to prolong the maturation defect, which suggests that this pathogen is uniquely adapted to the CF environment (Lamothe and Valvano, 2008).

1.5 - Bacterial Secretion Systems

Complex host-pathogen interactions such as the induction of a host phagosome maturation delay, pathogen invasion, or induction of host cell death, are common consequences of bacterial infection. Gram-negative bacteria commonly employ multi-protein complexes that secrete or translocate effector proteins into host cells. These effectors interfere with key components of cellular signaling pathways.

The multi-protein complexes, or secretion systems, are numbered chronologically based on their order of discovery. The secretion systems are subdivided into two broad groups: 1) contact-dependent; and 2) non-contact-dependent systems. Contact-dependent systems can ultimately deliver effectors from the pathogen's cytoplasm directly into the cytoplasm of the host cell. Non-contact-dependent systems transport effectors across the double membrane envelope of the Gram-negative pathogen, and do not translocate effectors directly across host cell plasma membranes. Figure 1 depicts the classical secretion systems.

Figure 1: Overview of the five original secretion systems known in Gram-negative bacteria. Depicted are five secretion systems, listed in order, with corresponding protein names for the bacterial species with the best characterized example of each. T3SS and T4SS transport effector molecules directly from the bacterial cytoplasm into host cytoplasm (i.e. translocation) whereas all other secretion systems secrete effectors into the extracellular space (with the exception of the T6SS, not shown in this diagram. For extensive review of protein names from each pathogen, refer to Gerlach and Hensel, 2007 the study from which this diagram has been adapted.

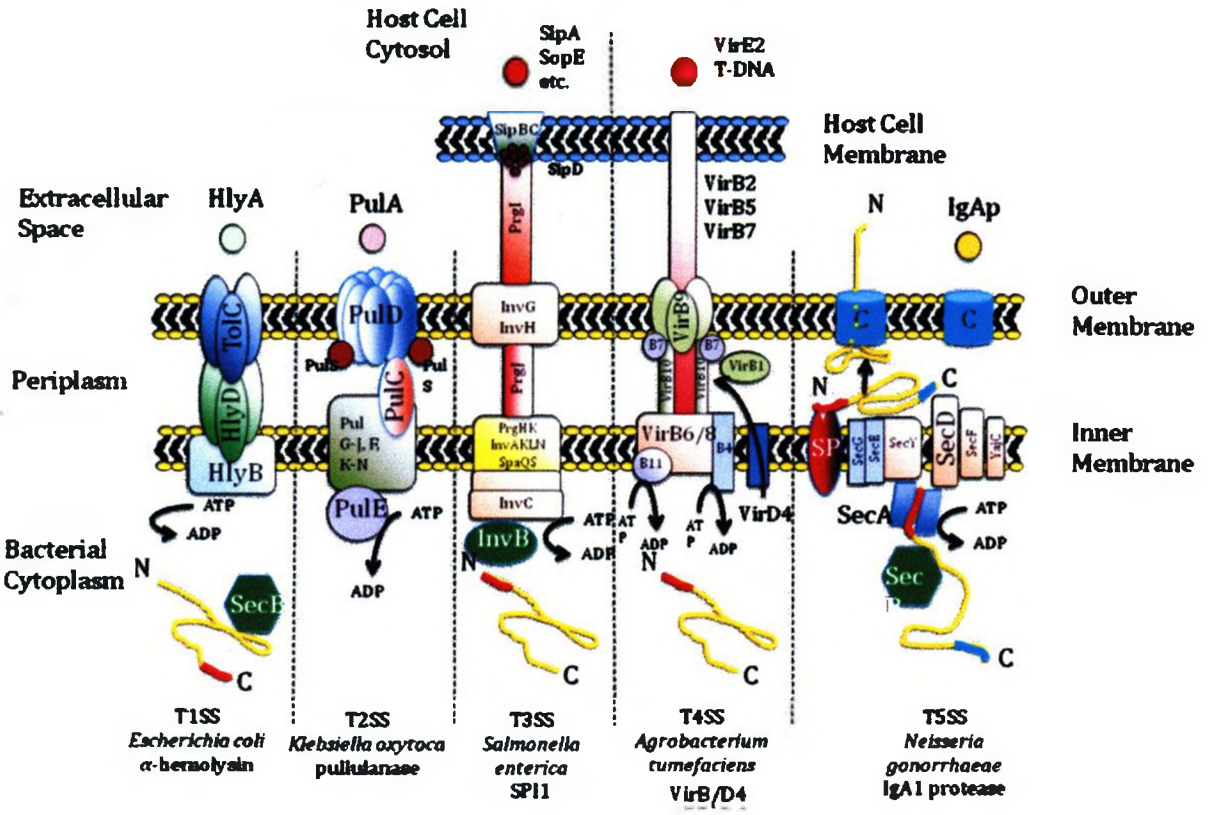
Host Cell
Cytosol
SipA
SopE
etc.
VirE2
T-DNA
Host Cell
Membrane
Extracellular
Space
HlyA
PulA
VirB2
VirB5
VirB7
N
IgAp
Outer
Membrane
Periplasm
Inner
Membrane
ATP
ADP
Bacterial
Cytoplasm
SecB
SecA
VirD4
T1SS
Escherichia coli
α-hemolysin
T2SS
Klebsiella oxytoca
pullulanase
T3SS
Salmonella
enterica
SPI1
T4SS
Agrobacterium
tumefaciens
VirB/D4
T5SS
Neisseria
gonorrhaeae
IgA1 protease

1.5.1 - Non-Contact-Dependent Secretion Systems:

1.5.1.1 - Type 1 Secretion Systems: ABC-Exporter

Type 1 secretion systems enable Gram-negative bacteria to export unfolded proteins directly from the bacterial cytoplasm into the extracellular space without a periplasmic intermediate (Wandersman *et al.,* 1987). Three integral proteins crucial to this process are: 1) an ABC-binding cassette located in the inner-membrane which identifies a suitable effector via the recognition of a specialized signal peptide, 2) a membrane fusion protein (MFP) which establishes a connection between components found in the inner and outer membranes, and 3) an outer membrane protein (OMP) which forms a long channel originating at a constricted periplasmic tip, running through the outer membrane, and out into the extracellular space (Delepelaire, 2004). A prototypic Type 1 secretion system is the *E. coli* alpha-hemolysin (HlyA). Components of the HlyA T1SS include the ABC transporter HlyB, the MFB HlyD, and the common OMP TolC (Schulein *et al.,* 1992; Koronakis *et al.,* 2000). HlyD is believed to interact with TolC within the periplasm, possibly to trigger the opening of TolC channel, allowing the passage of HlyA into the extracellular milieu (Koronokais *et al.,* 2000; Gerlach and Hensel, 2007). Once secreted, HlyA inserts into the host cell membrane, forms a pore, and ultimately releases intracellular contents through cytolysis and causes inflammation (Gentschev *et al.,* 2001).

1.5.1.2 - Type 2 Secretion System: General Secretory Pathway

Secretion via the T2SS utilizes two distinct membrane translocation mechanisms, one for each membrane of the Gram-negative double membrane envelope. Widely referred to as the main terminal branch (MTB) of the general secretion pathway, the secretion products or effectors result in pathogenesis in the host cell. This mode of effector secretion has been demonstrated in both plant and animal host cells, with plant pathogens typically secreting cellulase and pectinase, and animal pathogens secreting proteases and toxins (van Bueren *et al.,* 2007). Depending on the specific system, 12 to 14 proteins may be involved in the T2SS export of effector proteins. The best characterized T2SS is in *Klebsiella oxytoca,* and is responsible for the secretion of pullulanase (PulA) (Pugsley *et al.,* 1997). The secretory machine consists of multiple subunits inserted into the inner membrane (Sandvkist *et al.,* 1995). The T2SS proteins PulG, H, and I are homologous to the pilin subunit of the T4SS pilus (Gerlach and Hensel, 2007). Effector proteins are exported across the inner membrane into the periplasm via the general secretion pathway, or Sec (Gerlach and Hensel, 2007). Once in the periplasm, the effector proteins fold into mature forms and they undergo multi-protein complex formation prior to export across the outer membrane (Sandvkist, 2001; Gerlach and Hensel, 2007). This periplasmic maturation step provides the most distinctive difference between T2SS and other types because mature effectors are eventually transported across the outer membrane.

The T2SS takes the form of a pore in the outer membrane and pilus anchored to the cytoplasmic side of the inner membrane directly opposite to the pore, with

the pilus possibly providing mechanical force to extrude effector proteins out of the periplasm (Sandvkist, 2001; Gerlach and Hensel, 2007). The T2SS pilus is similar to the T4SS pilus, with proteins sharing homology to T4SS pilus biogenesis proteins (Nunn, 1999). Specifically, accessory genes needed for assembly of the Type IV pilus are homologous to T2SS genes. Interestingly, the *Vibrio cholerae ctxAB* genes encoding cholera toxin (which is secreted by the T2SS) are carried on a lysogenic phage. This CTX phage utilizes conjugative type IV pilus as a receptor to gain access to bacterial cytoplasm (Waldor & Mekalanos, 1996).

1.5.1.3 - Type 5 Secretion System: The Auto-Transporter

There are three sub-classes of T5SS: Auto-transporter (AT) secretion, the two-partner (TPS) system, and an oligomeric coiled-coil adhesin (Oca) system (Gerlach and Hensel, 2007). The AT secretion mechanism was the first method to be characterized and is the simplest of the known secretion systems. The AT mechanism was first discovered in *Neisseria gonorrhaeae* (Pohlner *et al.,* 1987). The transport system and the substrate protein are synthesized as a single protein that contains an N-terminal leader domain, a secreted functional domain, and a C-terminal "helper" domain (Pohlner *et al.,* 1987). The leader domain enables transport across the inner membrane via the general secretory pathway. The "helper" domain is a pore-forming domain that enables transport of the functional domain across the outer membrane (Gerlach and Hensel, 2007). Through this mechanism, the transit of the effector or auto-transporter is not energy coupled, which differentiates it from the other secretion systems. Important human

pathogens encoding a T5SS include *Shigella flexneri* and enteropathogenic *E. coli*, the latter of which encodes an EspC autotransporter (Gerlach and Hensel, 2007). EspC proteolytically cleaves host hemoglobin, liberating iron that is then used for bacterial growth (Schmidt and Hensel, 2004)

1.5.2 - Contact-Dependent Secretion Systems

1.5.2.1 - Type 3 Secretion System: The Needle

Like other members of the contact-dependent secretion system grouping, the pathogen requires close interaction with host cells before the T3SS becomes fully functional. Exceptions exist wherein the T3SS is 'leaky', but its efficient modulation still requires interaction with host cells (Cornelis, 2006). The T3SS effector proteins do not contain a cleavable signal sequence, as was noted with the T2SS. Instead T3SS effectors require protein chaperones for secretion to occur. The genes encoding T3SS subunits possess similarity to gene clusters encoding components of the flagellar apparatus and its biogenesis machinery (Cornelis, 2006). Interestingly, T3SS gene clusters found in plant pathogens have greater identity to flagellar gene clusters than do T3SS clusters obtained from animal pathogens (Jin and He, 2001). This suggests that the T3SS evolved first to modulate plant host cells, and following horizontal transfer or evolution of plant pathogens was then utilized to compromise animal host cells.

The quaternary structure of the T3SS resembles a 'needle' (Blocker *et al.*, 2001) with several highly conserved, core components which are subdivided into two groups: 1) outer membrane proteins and lipoproteins, and 2) a group sharing

distinct homology to flagellar export apparatus (Cornelis, 2006). The needle acts as a puncturing device with a hollow conduit on the inside, which allows for the transport of proteins.

Animal pathogens such as *Salmonella enterica* serovar Typhimurium (*S. typhimurium*) and enteropathogenic *Escherichia coli* use the T3SS in different ways. *S. typhimurium* uses its T3SS to gain access to non-phagocytic epithelial cells through the induction of host cell 'membrane ruffling' via modulation of the actin cytoskeleton (Cain *et al.,* 2004). In the case of *E. coli,* the pathogen utilizes its T3SS and secretion of the effector EspF in order to disrupt normal PI-3 kinase function and phagocytosis (Quitard *et al.,* 2006). PI-3 kinase is crucial to phosphorylation events that mediate phagocytosis (Cox *et al.,* 1999). By remaining extracellular and adherent, the pathogen exerts modulating effects from the exterior surface of the host cell membrane (Quitard *et al.,* 2006).

1.5.2.2 - Type 4 Secretion System: Dot/Icm

Type 4 secretion systems share characteristics with bacterial conjugative pili, and secrete effectors either to the extracellular milieu or translocate them directly into host cell cytosol (Gerlach and Hensel, 2007). The effectors can be either proteins or protein-DNA complexes. One of the most well characterized T4SS mediates the secretion of pertussis toxin (Ptl) by *Bordetella pertussis.* Ptl consists of two domains, A and B (Malaisse *et al.,* 1984). The T4SS of *B. pertussis* does not modulate host cells through translocation of effectors, but rather secretion of Ptl into the extracellular space, where the B domain of the toxin interacts with

glycoprotein receptors on the surface of the host cell. Host glycoprotein receptors then allow access of the A domain into the host cell cytosol, where it modifies host G-proteins through ribosylation (Malaisse *et al.,* 1984).

Upon internalization by the host cell, *L. pneumophila* rapidly modifies its vacuolar compartment, departs the classical phagosome maturation pathway and surrounds its compartment with rough endoplasmic reticulum (Horwitz, 1983). *L. pneumophila* modifies the intracellular compartment via a T4SS (Bardill *et al.,* 2005). Following modification of the intracellular compartment, caspase-3 mediated apoptosis is induced (Gao and Kwaik, 1999). Intracellular bacteria enter an exponential growth phase, which is a major hallmark of Legionnaire's disease (Kwaik, 1998). Once this growth reaches a plateau, a pore-forming toxin is secreted by the T4SS, host cells are rapidly lysed, and *L. pneumophila* escapes into the extracellular space, perpetuating infection into neighbouring cells (Kirby *et al.,* 1998). The T4SS of *L. pneumophila* is dependent on the accessory proteins IcmF and DotU (or IcmH), which stabilize the secretion apparatus and normal effector translocation (Bandyopdahyay *et al.,* 2004). T4SS mutants are unable to modify host phagosomes, do not undergo intravacuolar growth, and cannot mediate cytolytic escape from the host cell.

1.5.2.3 - Type 6 Secretion System

Components of the Type 6 Secretion System (T6SS) were first discovered in *P. aeruginosa* (Mougous *et al.,* 2006) and in *V. cholerae* (Pukatzki *et al.,* 2007). Strain V52 of serogroup O37 of *V. cholerae* was known at the time to lack functional

secretion systems yet evaded predatory killing by the eukaryote when plated along with predatory amoeba *Dictyolstelium discoideum* (Pukatzki *et al.,* 2007). Strain V52 has an *icmF* homologue even though it does not have a known T4SS (Das and Chaudhuri, 2003). Transposon mutagenesis identified this *icmF* homologue and other genes found within a virulence associated secretion (*vas*) gene cluster that were required to escape amoeboid killing (Pukatzki *et al.,* 2007).

In certain species, at least two key structural components, hemolysin co-regulated protein (Hcp) and valine glycine repeat (Vgr) proteins, also function as effectors. Recently, the AAA-ATPase ClpV was shown to function as the engine driving machinery through the hydrolysis of ATP, but this enzyme is also involved in the cleavage of unique tubular structures composed of the proteins VipA and VipB. Cleavage of these bacterial "microtubules" is necessary for function of the T6SS in at least one bacterial species (Bonemann *et al.,* 2009), and is an unprecedented mechanism among bacterial secretion systems. The T6SS contains unique components, which are continuing to be discovered at an impressive rate. Despite this, a dedicated T6SS effector protein has not been described in any Gram-negative species. The T6SS's function is unique to each bacterial species that expresses the system. Importantly, in all but a few rare instances, the T6SS is linked to pathogenesis.

The gene clusters encoding T6SS of different species are typically found within pathogenicity islands (Cascales, 2008) but unlike other secretion systems, the G+C content of these islands does not differentiate greatly from the rest of the bacterial chromosome (Cascales, 2008). This suggests that horizontal transfer was

not a recent event, and that acquisition of the T6SS is a more ancient event. Like the T3SS and T4SS, the fact that the gene clusters may have been transferred in the distant past may explain the variety of roles these secretion systems play. Over time, genetic recombination introduced genes into these systems and modified their expression to suit the needs of the bacterium.

T6SS are typically found within a pathogenicity island, or on chromosomes that show a bias toward virulence or survival within a host (Cascales, 2008). Also, in at least one species, *P. aeruginosa,* three encoded T6SS clusters were acquired at separate times during the evolution of that organism, suggesting that acquisition of multiple, functional copies of this secretion system may provide a selective advantage to a species (Bingle *et al.,* 2008). Most other bacterial species encoding a T6SS have multiple copies, but only *P. aeruginosa* has multiple copies proven to have separate evolutionary origins (Bingle *et al.,* 2008).

Among the gene clusters there are many genes that are specific to different species. However, there is a growing list of genes that are common to all T6SS and are therefore hallmarks of this recently discovered secretion system. Figure 2 summarizes these components in a proposed model.

1.5.2.3.1 - IcmF homologues

IcmF protein homologues are important for T6SS function, and share homology to critical accessory proteins of the T4SS. For example, IcmF and DotU (or IcmH) were originally identified as accessory proteins of the T4SS in *L. pneumophila* (Horwitz, 1983). However, a homologue of IcmF is broadly conserved throughout

many bacterial species, but is not associated with other known T4SS genes (Das and Chaudhuri, 2003). The IcmF associated homologous protein cluster (IAHP) discovered in *V. cholerae, P. aeruginosa, Yersinia pestis, L. pneumophila, E. coli* and *S. typhimurium* forms part of the T6SS gene cluster. The protein is predicted to have a transmembrane region, a large periplasmic domain and a cytosolic domain (Bonemann *et al.,* 2009). The cytosolic domain contains a Walker A motif, suggesting that IcmF may be involved in or share energy-coupling responsibilities in order to drive effector translocation through the T6SS apparatus (Bonemann *et al.,* 2009).

1.5.2.3.2 - VgrG

Pukatzki *et al.* (2006) found that strain V52 of *V. cholerae* lacked both a T3SS and a T4SS but still encoded an IAHP cluster, which contained homologues of genes crucial to the T4SS of *L. pneumophila.* Pukatzki *et al.* (2006) also determined that genes within this cluster were necessary for the bacterium to evade predation by *D. discoideum,* a predatory amoeba. The IAHP cluster, or virulence-associated secretion *(vas)* cluster, encodes homologues of Hcp and Vgr proteins (Pukatzki *et al.,* 2007). The deletion of only one of the Vgr proteins, VgrG-1, resulted in loss of T6SS function and Hcp secretion. It was also found that the C-terminal domain of VgrG-1 was homologous to a functional actin-crosslinking domain (ACD) of the RTXa toxin of *V. cholerae.* This C-terminal domain of VgrG-1 is involved in the cross-linking activity of the V52 strain and its ability to escape predation by *D. discoideum.*

Figure 2: Proposed model of T6SS function. The T6SS complex spans the bacterial cell envelope and punctures the host cell membrane. Components of the T6SS, namely VgrG and Hcp, can be found as part of the secretion complex and also secreted effectors. Known effectors for all species have yet to be discovered, but would likely exit through the central channel of the VgrG/Hcp proteins of the apparatus. Within the bacterial cytoplasm, PpkA phosphorylation of a threonine residue present on FHA results in activation of this protein. PpkA is also involved in export of Hcp across the outer membrane of bacteria, as loss-of-function mutations in *ppkA* caused accumulation of Hcp in the periplasm. PppA antagonizes PpkA function when stimulus is insufficient to require T6SS expression. Upon activation, FHA causes the clustering and oligomerization of ClpV monomers, resulting in the oligomeric ClpV ring. Within this ring, two pores exist (only one depicted). VipA/VipB tubules are threaded through the ClpV pore, resulting in cleavage of long tubules into shorter VipA/VipB tubules. This cleavage has been shown to be necessary for T6SS secretion of VgrG and Hcp into the host cytosol. ClpV somehow coordinates these cleavages with the usage of ATP to drive the assembly of the T6SS machinery, and may or may not be assisted by the presence of IcmF proteins within the inner membrane. A number of proposed periplasmic structural components have yet to be discovered (indicated by question marks). The Δ*hcp* mutant used in this study lacks the primary conduit of the T6SS comprised of Hcp monohexameric rings, and therefore, the T6SS is non-functional. The Δ*atsR* mutant used in this study has been shown to hyper-secrete Hcp proteins, and is believed to over-express all components of the T6SS depicted in this model.

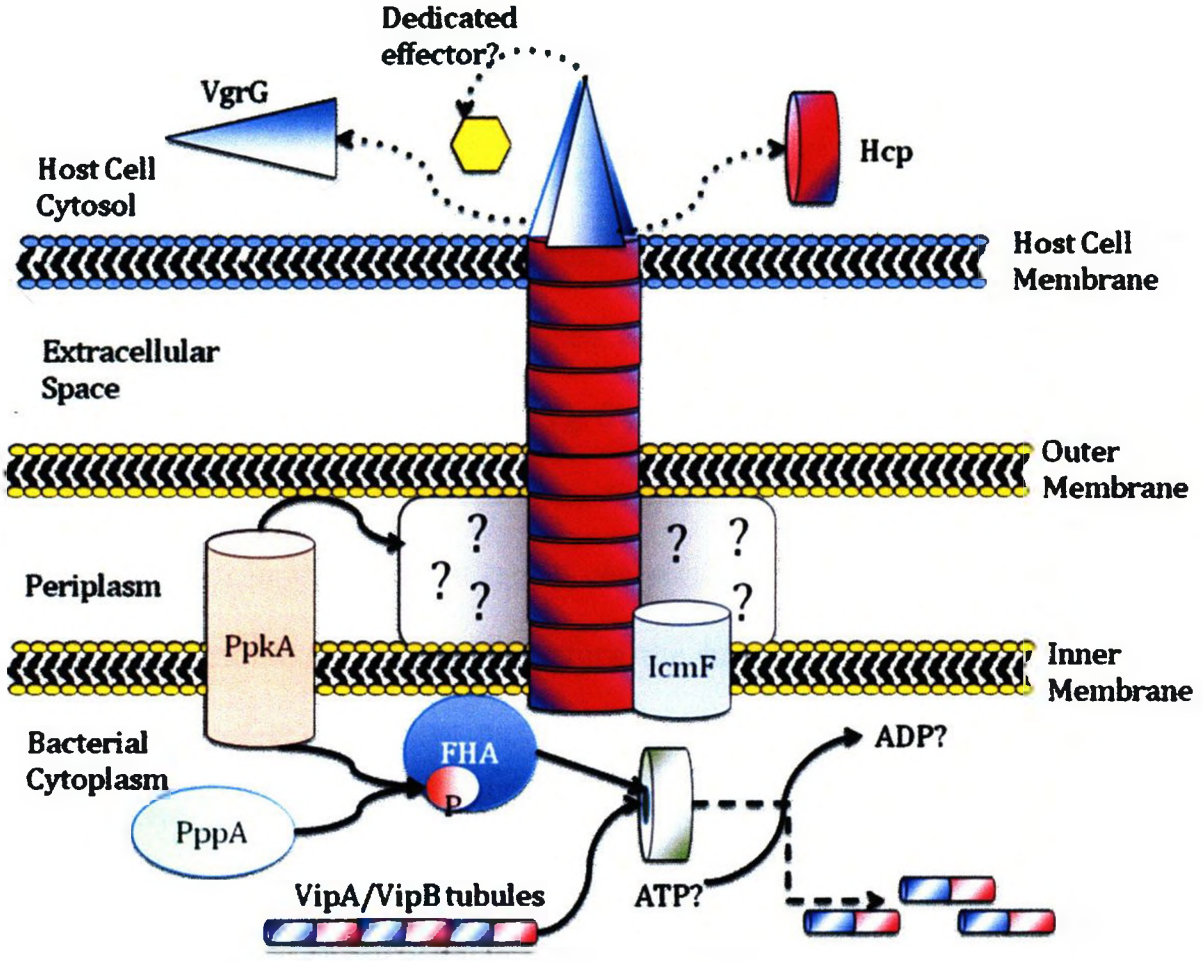
Dedicated
effector?
VgrG
Host Cell
Cytosol
Hcp
Host Cell
Membrane
Extracellular
Space
Outer
Membrane
Periplasm
PpkA
IcmF
Inner
Membrane
Bacterial
Cytoplasm
FHA
P
ADP?
PppA
VipA/VipB tubules
ATP?

Therefore, VgrG-1 proved to be a necessary component of the machine structure as well as a secreted effector required for virulence (Pukatzki *et al.,* 2007).

VgrG homologues have been discovered in other species; some encode a predicted functional C-terminal domain, while others do not (Pukatzki *et al.,* 2007). The functional C-terminal domains can vary drastically among VgrGs from different bacteria. For example, the VgrG proteins of *A. hydrophilia* contain a ubiquitin-like domain suggested to interfere with host cell protein synthesis, and the C-terminus of VgrG-1 from *V. cholerae* contains a functional ACD. A current theory of the T6SS is that a nanotube of Hcp rings functions as the central conduit for the secretory apparatus, and a trimeric complex of VgrG proteins is found at the growing tip of the apparatus. In some cases, there is a functional domain at the C-terminal end of the VgrG trimer, for instance, the ACD of *V. cholerae* strain V52. In other species, the tip of the VgrG trimer may simply puncture the host cell membrane and dedicated effector molecules may enter into the host cytosol through the Hcp-mediated conduit. The cell puncturing mechanism has yet to be demonstrated experimentally.

1.5.2.3.3 - Hcp

Hcp and VgrG proteins are the first two components discovered to be involved in the T6SS machinery. Hcp forms monohexameric rings with a channel diameter of 4.0-nm (Ballister *et al.,* 2008) and spontaneously forms nanotubes when purified in solution (Ballister *et al.,* 2008). These nanotubes can grow to 0.1-μm via the intrinsic chemical complimentarity of their amino acid residues, and through experimental engineering of disfulfide bonds (Ballister *et al.,* 2008). Despite lacking significant

sequence similarity, when Hcp homologues from different bacterial species are purified and coincubated *in vitro*, they form channels due to the quaternary structure of Hcp (Pell *et al.*, 2009). The organization of Hcp monomers into a functional conduit via self-assembly in the absence of ATP may reduce the overall energy required by a pathogen to produce a T6SS (Ballister *et al.*, 2008).

In vivo, Hcp is believed to form a lengthening tube that transits the bacterial inner membrane, periplasm, outer membrane, and the host cell membrane. From this position, it may transfer effectors through its interior channel into the host cytosol.

1.5.2.3.4 – Homology to phage proteins: gp5, gp25, and gp27

The common evolutionary origin shared between a group of T6SS components and the tail-associated protein complexes of bacteriophage suggests that VgrG proteins function as a spike (Leiman *et al.*, 2009). An N-terminal fragment of a VgrG protein from *E. coli* shared structural similarity with the gp5-gp27 complex found in nearly all long-tailed bacteriophage (Leiman *et al.*, 2009). Furthermore, Hcp of *P. aeruginosa* is homologous to the phage tail tube protein of bacteriophage, and that Hcp is in fact a structural homolog of gp5 from bacteriophage lambda (Pell *et al.*, 2009). Lastly, the gp25 protein is found throughout nearly all phages that encode contractile tails, and this protein is necessary to connect central and peripheral parts of baseplates found in contractile tails. A variety of gene clusters encode a gp25 homologue, which proves that the T6SS is related to bacteriophage tail-spike complexes. These data suggest more strongly that the T6SS resembles a contractile

spike complex capable of puncturing host cell membranes, similar to bacteriophage contractile tails.

1.5.2.3.5 – ClpV AAA+ ATPase

A sub-family of Clp AAA+ ATPase enzymes, ClpV proteins, is important to bacterial secretion systems within known human pathogens (Schlieker *et al.,* 2005). Generally, the Clp family of ATPases is necessary for the disaggregation and degradation of misfolded proteins within prokaryotic cells and uses ATP to carry out these functions (Zolkiewski, 2006). ClpV ATPases differ from other Clp superfamily members due to their to form oligomeric complexes which are not capable of protein disaggregation activity, but are necessary for the normal functioning of associated secretion systems (Schlieker *et al.*, 2005).

A ClpV AAA+ ATPase is always associated with functional T6SS gene clusters, and it may be required for the translocation mechanism of T6SS effectors or the assembly of the complex (Bonemann *et al.,* 2009). Indeed, ATP-hydrolysis mediated by ClpV may provide the driving force for machine assembly, for protein secretion, or for both processes. In *P. aeruginosa,* ClpV proteins tagged with GFP, which also remain functional, become localized in discrete regions of the bacterial cells. These clusters depend on the expression of Hcp, IcmF, and FHA proteins. The phosphorylation activities of a serine-threonine kinase, PpkA, are also necessary (Mougous *et al.,* 2006). The N-terminal domain found in ClpV subfamily members is specific to that group, and is not found within members of other subfamilies of Clp AAA+ ATPases. Moreover, ClpV is required for the export of conserved Hcp and

VgrG proteins, but does not act on these proteins directly. Rather, ClpV interacts with two proteins which form a novel cytosolic tubular structure and which are encoded in all T6SS gene clusters (Bonemann *et al.,* 2009).

1.5.2.3.6 - ClpV interacting proteins

An unusual characteristic of ClpV ATPases is the binding of its specific N-terminal domain to other proteins encoded by the *vas* cluster of *V. cholerae,* designated ClpV-interacting proteins (VipA and VipB) (Bonemann *et al.,* 2009). These proteins are conserved throughout all presently known T6SS clusters. Bonemann *et al.* (2009) demonstrated that in solution, and in the presence of ATP, VipA and VipB associated to form large tubular complexes in excess of 2000 kDa. Following introduction of purified ClpV to this solution, the ATPase remodeled these tubules to not exceed 80 kDa, and these smaller tubules still contained both Vip proteins. VipB appears to drive the formation of these tubules, as VipA alone could not form these structures. These proteins were not found in cell-culture supernatants, and therefore do not appear to be secreted. The remodeling of large VipA/VipB tubules is carried out via threading of the tubule through one of two pores in the ClpV oligomer. When key residues were mutated within that pore, threading of VipA/VipB tubules did not occur. Most importantly, in the absence of a functional pore for ClpV threading, Hcp and VgrG proteins were both not secreted. This indicates that VipA/VipB threading and ClpV remodeling of these tubules is critical for normal T6SS function. The presence of these tubules is a novel finding

among secretion systems, as is the existence of an AAA+ ATPase associated with a secretion apparatus.

1.5.2.3.7 - PpkA/PppA and FHA

Threonine phosphorylation regulates T6SS in *P. aeruginosa* (Mougous *et al.,* 2007). The unprecedented phosphorylation of a threonine residue in a bacterial species results from the activity of the kinase PpkA and is antagonized by the phosphatase PppA. The primary target of PpkA phosphorylation is the fork-head association (FHA) protein. The amount of p-FHA present in the bacterial cell correlates with the degree of Hcp secretion among clinical isolates of *P. aeruginosa* (Mougous *et al.,* 2007). Furthermore, sufficient p-FHA results in clustering of ClpV, allowing for ClpV oligomerization and subsequent cleavage of VipA/VipB tubules (Bonemann *et al.,* 2009). In the absence of PpkA, Hcp is only secreted into the periplasm, suggesting that PpkA activity is also involved directly in the translocation of effectors across the outer membrane (Mougous *et al.,* 2007). The identification of threonine phosphorylation was a critical step in understanding the complex regulation of the T6SS cluster.

1.5.2.3.8 - RetS regulation and AtsR

The T6SS in *P. aeruginosa* is positively regulated by LadS and negatively regulated by RetS (Mougous *et al.,* 2006). The T3SS is under opposing regulation by these two proteins (Laskowski and Kazmierczak, 2006). T3SS is commonly expressed during acute infection while the T6SS has been connected with chronic

infection. The reciprocal regulation model enables a pathogen to express genes that are appropriate to either acute or chronic infection scenarios. RetS is considered an important sensor-kinase response regulator hybrid necessary to switch *P. aeruginosa* virulence from acute to chronic infection modalities (Laskowski and Kazmierczak, 2006). Generation of a RetS mutant releases the T6SS and biofilm formation from negative regulation, and results in the attenuation of *P. aeruginosa* virulence due to mistiming of gene expression (Goodman *et al.,* 2004).

In *B. cenocepacia,* a RetS homologue was discovered and named AtsR (adhesion and type six regulator). This protein is a sensor-kinase response regulator hybrid (Aubert *et al.,* 2008). Insertional inactivation or deletion of *atsR* results in increased biofilm formation and constitutive expression of the T6SS, as suggested by the secretion of Hcp into cell culture supernatant. AtsR-mutant bacteria experienced reduced predation by *D. discoideum,* and induced the a robust phenotype in the ANA-1 murine macrophage cell line (Aubert *et al.,* 2008). The effect of *atsR* inactivation and overexpression of the T6SS on murine macrophages was the induction of irregular membrane protrusions around the periphery of infected cells, which were absent following infection with a strain lacking a functional T6SS through deletion of *hcp*. These protrusions stained strongly with the actin-binding fungal toxin phalloidin (Aubert *et al.,* 2008). The modification of the host cell actin cytoskeleton is of particular interest; given the role that actin is known to have in vesicle trafficking and fusion of endosomes with a maturing phagosome (Kjeken *et al.,* 2004).

1.6 – Phagosome maturation

Shortly after phagocytosis, the lumen of the phagocytic vacuole is similar to the extracellular milieu. However, the phagosome undergoes sequential fusions with vacuoles of the endocytic pathway, resulting in a progressive pH decrease, and enrichment of hydrolytic enzymes of the cathepsin family, particularly after fusion with the lysosome (Desjardins *et al.,* 1994). Antimicrobial factors include reactive oxygen species introduced through a fully assembled NADPH oxidase complex on the membrane of the phagosome, as well as reactive nitrogen species due to assembly of the inducible nitric oxide synthase (iNOS) (Keith *et al.,* 2009). The reduction in pH is caused by the recruitment of vacuolar ATPase enzymes to the phagosomal membrane. As these enzymes gradually accumulate the phagosomal lumen develops a pH of 4.5 (Lukacs *et al.,* 1990).

Simplified stages of phagosomal maturation have been described for the maturing phagosome and include: early phagosome, late phagosome, and phagolysosome. The small GTPases Rab5 and Rab7 regulate the stages of phagosome maturation in this model (Vieira *et al.,* 2002). Rab5 coordinates early to late phagosome progression through recruitment of the early-endosomal auto-antigen (EEA1). Rab7 facilitates the recruitment of lysosome-associated membrane proteins (LAMPs), which in turn facilitate the end-stage fusion event with the lysosome (Huynh *et al.,* 2007). These stages of phagosome maturation are summarized in Figure 3.

Bacterial species have numerous ways of compromising phagosome maturation, ranging from pathway stoppage, to redirection of vacuoles into other

Figure 3: Standard model for phagosome maturation. Phagosomal stages progress based on the activity of the Rab GTPases, Rab5 and Rab7. Rab5 activity results in the progression to early-phagosome, while Rab7 activity enables the maturation from early-phagosome to late-phagosome. Acquisition of LAMPs denotes the maturation from late-phagosome to fusion with the lysosome, producing the phagolysosome. The typical timeline for complete maturation of the phagosome is approximately 40-60 minutes following phagocytosis. Adapted from Vieira *et al.,* 2002.

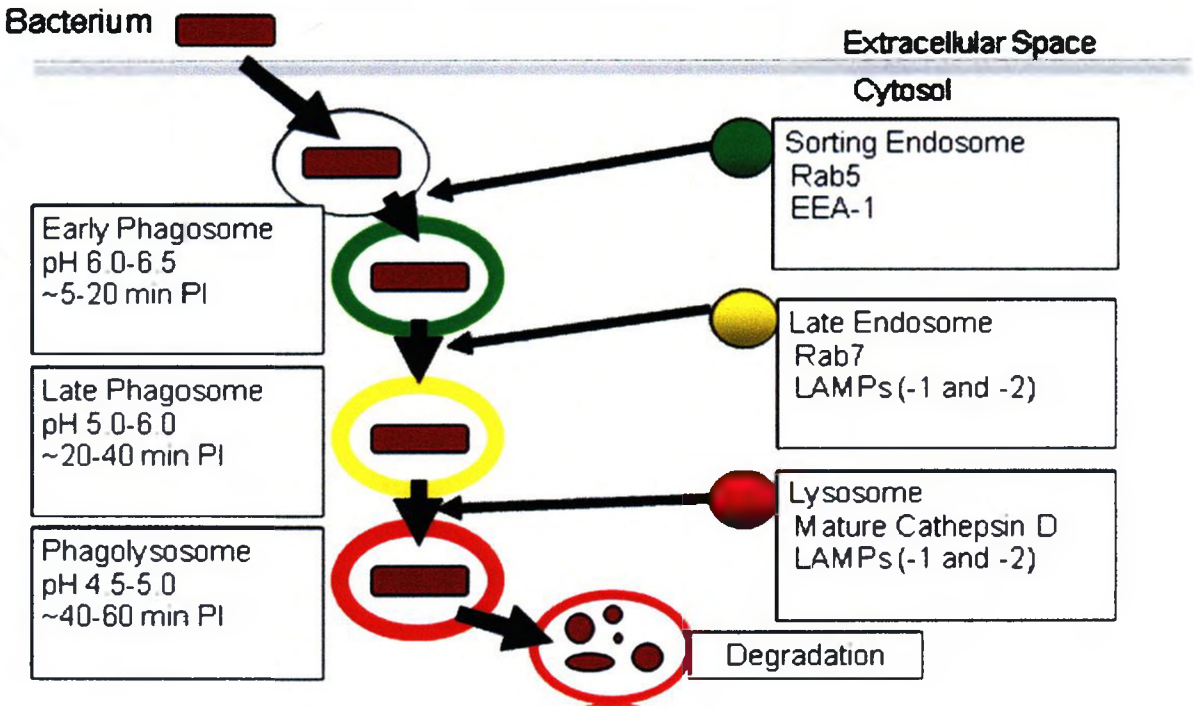
Bacterium
Extracellular Space
Cytosol
Sorting Endosome
Rab5
EEA-1
Early Phagosome
pH 6.0-6.5
~5-20 min PI
Late Endosome
Rab7
LAMPs (-1 and -2)
Late Phagosome
pH 5.0-6.0
~20-40 min PI
Lysosome
Mature Cathepsin D
LAMPs (-1 and -2)
Phagolysosome
pH 4.5-5.0
~40-60 min PI
Degradation

vesicle trafficking pathways, to simply degrading the phagosome membrane and existing in the host cell cytosol. In the case of *B. cenocepacia*, Lamothe *et al.* (2007) described a phenomenon mediated by live *B. cenocepacia* strain J2315 that enables the bacterium to prolong the maturation process between early and late phagosome stages. The phenomenon is characterized by loss of EEA-1 and lack of recruitment of LAMP-1 around bacteria-positive vacuoles after phagocytosis by RAW 264.7 macrophages. Approximately six hours later, approximately 75% of bacteria can be found localized within LAMP-1 rich vacuoles. Other groups have noted that *B. cenocepacia* containing vacuoles recruit markers of autophagy (Sajjan *et al.,* 2006). The model describing *B. cenocepacia* induced delay of phagosome maturation is illustrated in Figure 4.

1.7 - Cytoskeletal remodeling

Normal function of the actin cytoskeleton is crucial to the function of host cells. The cytoskeleton is directly involved in maintaining cell shape and enabling migratory behaviour. The actin cytoskeleton is also involved in vesicle trafficking within the cytosol, especially between the phagosome and the endosomal pathway (Kjejen *et al.,* 2004). The actin cytoskeleton is tightly regulated by at least 100 different proteins (Dos Remedios *et al.,* 2003). Invading bacteria can interfere with the actin cytoskeleton. For example, *S. typhimurium* induces ruffling of the host cell membrane via manipulation of the actin cytoskeleton, which facilitates the pathogen's entry into epithelial cells (Cain *et al.,* 2004). Other pathogens like *Listeria monocytogenes* gain access to the cytosol and co-opt monomeric actin resulting in

Figure 4: Phagosome maturation delay induced by internalized *B. cenocepacia*. Internalized *B. cenocepacia* induces a delay in the acquisition of phagosomal markers by an unknown mechanism. Characteristics of the *B. cenocepacia*-containing vacuole include normal EEA-1 acquisition, six-hour delay in LAMP-1 recruitment, deficient acidification mediated by the V-ATPase, delayed assembly of the NADPH-oxidase, and prolonged intracellular bacterial survival. Adapted from Lamothe *et al.,* 2007.

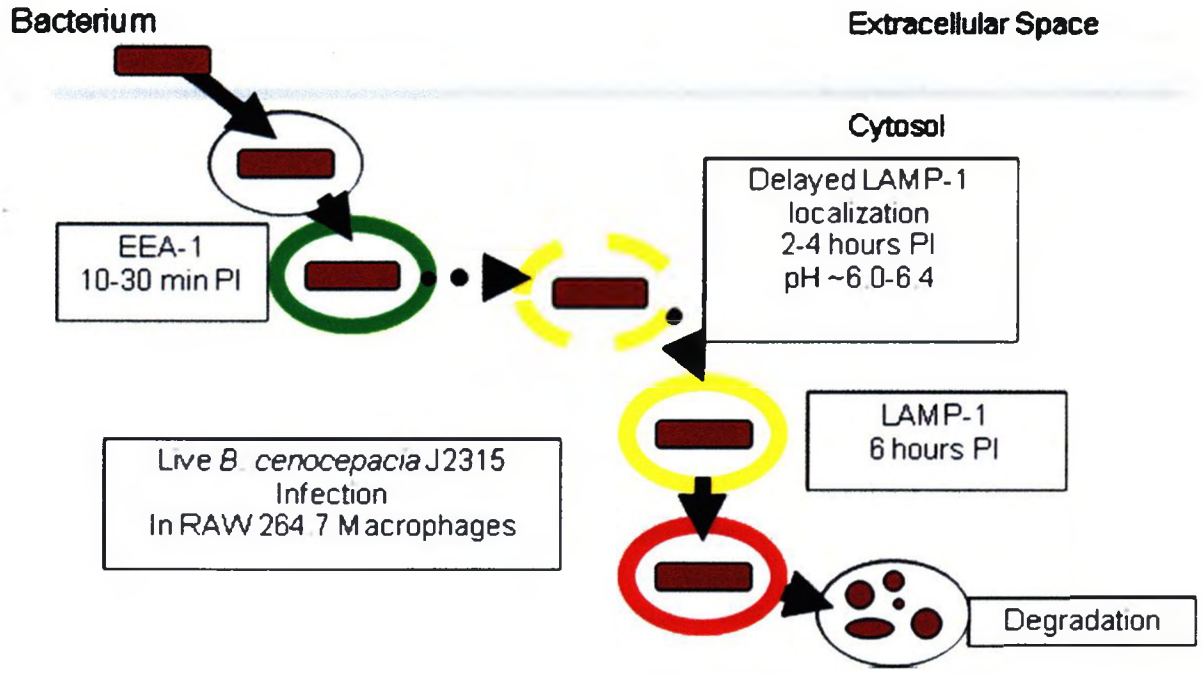
Bacterium
Extracellular Space
Cytosol
EEA-1
10-30 min PI
Delayed LAMP-1
localization
2-4 hours PI
pH ~6.0-6.4
LAMP-1
6 hours PI
Live B. cenocepacia J2315
Infection
In RAW 264.7 Macrophages
Degradation

the characteristic "actin comet tailing" of this bacterium and its ability to pass from cell to cell without re-entering the extracellular space (Cicchetti *et al.,* 1999).

1.8 - Caspase-3-dependent cell death

Following infection by bacterial pathogens, host eukaryotic cells often undergo one form of cell death or another. Cell death can be both caspase-dependent and caspase-independent, with one commonly induced mode of cell death being caspase-3-dependent programmed cell death, or apoptosis. Caspase enzymes were first described with the discovery of Ced-3 in *Caenorhabditis elegans,* a caspase enzyme crucial to normal development and the primary enzyme involved in cell death in that organism (Ellis and Horvitz, 1986). Mammalian homologues were discovered, and the list has expanded to 14 caspase enzymes in mammals. (Thornberry *et al.,* 1998). Caspase-3 is considered the canonical enzyme catalyzing programmed cell death via apoptosis, and its activity is required for the characteristic apoptotic chromatin condensation associated with this form of cell death (Porter and Jänicke, 1999).

Like other caspase enzymes, caspase-3 activity results from the proteolytic cleavage of the zymogen, pro-caspase-3, and the generation of a functional tetramer (Abraham and Shamam, 2004). The cleavage site for caspases is a tetrapeptide found within the substrate protein, which varies depending on the specific caspase. Caspase-3 and caspase-7 share an aspartic acid-glutamic acid-valine-aspartic acid (DEVD) tetrapeptide on their respective substrates, while specific substrate proteins can have specific tetrapeptide targets, such as protein kinase Cγ and its

aspartic acid-methionine-glutamine-aspartic acid (DMQD) tetrapeptide targeted by caspase-3. The subsequent activation of other caspases within the cell results in a cascade of proteolytic cleavage that ultimately results in controlled cell death. Substrates include the actin cytoskeleton, functional domains of other cellular enzymes, proteins of the nuclear envelope, and histones (Thornberry *et al.,* 1998).

One substrate that is crucial to the host differentiating apoptotic and non-apoptotic cells is the flippase enzyme that maintains phosphatidylserine (PS) membrane asymmetry (Daleke, 2003). A flippase enzyme limits this molecule to the inner leaflet of the cell membrane, but following caspase-3 activation, the flippase enzyme is cleaved and PS is flipped to the outer leaflet of the cell membrane. The presence of PS on the outer leaflet signals to neighbouring phagocytic cells to engulf the cell as its cellular contents undergo vesiculation as apoptotic bodies (or blebs). There is little consequence to neighbouring tissue because this process remains non-inflammatory, provided the apoptotic bodies are phagocytized in a timely manner and are not left to undergo secondary necrosis (Fink and Cookson, 2005).

Caspase-dependent cell death may occur through two signaling pathways, the extrinsic and the intrinsic pathways of caspase activation. The intrinsic pathway proceeds through permeabilization of the mitochondrial membrane. This process is mediated by the proteins Bax and Bak, which are normally inhibited by the anti-apoptotic Bcl-2 protein family (Degterev and Yuan, 2008). Bcl-2 family members reside in the mitochondrial outer membrane where they inhibit Bax and Bak. The anti-apoptotic effects of Bcl-2 are antagonized by Bcl-2 homology 3 (BH3)-only factors that bind Bcl-2 family members (Scorrano and Korsmeyer, 2003). Following

inhibition of anti-apoptotic Bcl-2 family members, Bax and Bak may form an oligomeric channel that leads to mitochondrial damage and cytochrome C release (Scorrano and Korsmeyer, 2003). Cytochrome C activates the protein Apaf, which through coordination with caspase-9 oligomerizes to form the multi-protein complex called the apoptosome, and this large protein complex then facilitates the activation of the executioner caspase-3 (Degterev and Yuan, 2008).

1.9 - Hypothesis

We hypothesized that the remodeling of host cell cytoskeleton caused by the T6SS may play a role in the phagosome maturation delay induced by *B. cenocepacia*. Also, knowing that infection with *B. cenocepacia* can culminate in necrotizing pneumonia, and the importance of the T6SS to other pathogenic bacteria, we hypothesized that the T6SS of *B. cenocepacia* may be involved in the induction of host cell death.

The specific objectives of this study were:

1 –To characterize the formation of the protrusion phenotype and to analyze the structure of the protrusions.

2 – To determine whether the T6SS is involved in delaying phagosome maturation.

3 – To determine whether the T6SS is involved in the induction of host cell death and, if so, attempt to define a mechanism through which cell death is induced.

Chapter 2

Materials and Methods

2.1 - Strains and plasmids

Strains and plasmids used in this study are listed in Table 2. Reagents used for bacterial growth were purchased from Sigma-Aldrich unless otherwise stated. Bacteria were grown at 37°C in Luria broth (LB). Broth cultures were grown overnight for approximately 16 hours with shaking. Bacteria were grown with antibiotics appropriate for the strain.

2.2 - Tissue culture reagents and fluorescent reagents used for microscopy

Dulbecco's modified eagle medium (DMEM) and fetal bovine serum (FBS), and phosphate-buffered saline (PBS) were obtained from Wisent (St. Bruno, Canada). Rat anti-LAMP-1 (ID4B) primary antibody (used in 1:50 dilution) was obtained from the Developmental Studies Hybridoma Bank (Iowa City, USA). Rabbit polyclonal primary antibody was generated against formalin-fixed *B. cenocepacia* bacteria, and during experimentation the antibody was used in a 1:500 dilution. Chicken anti-rat Alexa Fluor 488 secondary antibody, goat anti-rabbit Alexa Fluor 546 secondary antibody, 4',6-diamidino-2-phenylindole (DAPI), and Alexa Fluor 488-conjugated Phalloidin were obtained from Invitrogen: Molecular Probes. Fluoresbrite 2.00 μm YG Microspheres were obtained from Polysciences Inc (Warrington, USA).

2.3 - Cell death analysis reagents

Fluorescein-conjugated Annexin V and propidium iodide were obtained from Invitrogen: Molecular Probes. Saponin detergent and dimethyl sulfoxide (DMSO)

were obtained from Sigma-Aldrich Inc. Actinomycin D and Caspase-3 Inhibitor IV (Ac-DMQD-CHO) were obtained from Calbiochem.

2.4 - Macrophage and epithelial cell culture methods

Macrophages (ANA-1 or RAW 264.7) seed cultures were thawed from liquid nitrogen stocks and resuspended in DMEM with 10% FBS. The cell suspension was acclimated to growth conditions of 37°C at 5.0% CO_2 for one hour, and rinsed with pre-warmed PBS to remove dead macrophages and residual DMSO from the freezer stock. DMEM with 10% FBS growth media was then added to macrophages, which were incubated for a minimum of two days prior to first passage. Macrophages were sub-cultured at least once prior to use. Epithelial cell (A549) tissue culture methods were identical as for macrophages with the exception that these cells were subcultured once every 3-4 days.

2.5 - Bacterial infection of eukaryotic cells

One-milliliter aliquots from overnight bacterial cultures were dispensed in eppendorf tubes and spun at 16,000 x g for one minute. When heat-inactivated cultures were needed, prior to centrifugation, a one-milliliter aliquot of overnight broth culture was transferred to an eppendorf tube and placed in a 60°C water bath for 30 minutes. Following centrifugation, the supernatant was aspirated and the pellet was resuspended in 0.5 ml DMEM with 10% FBS. This process was repeated twice. After the final spin, the pellet was resuspended in 1.0 mL DMEM with 10% FBS. From this suspension, a 0.1-milliliter aliquot was prepared in a

Table 2: Bacterial strains and plasmids used in this study.

Strain or plasmid	Relevant characteristics	Source and/or reference
B. cenocepacia strains		
J2315	CF clinical isolate, clonal relative to K56-2 strain	BCRRC
K56-2	ET12 clone related to J2315, CF clinical isolate	BCRRC
DFA21	K56-2 *atsR*::pDA27; Tp^r: Over-expresses the T6SS	Aubert *et al.*, 2008
DFA27	K56-2 Δ*hcp*: Key T6SS structural protein not expressed, therefore, possesses a non-functional T6SS.	Aubert *et al.*, 2008
DFA21	K56-2 Δ*hcp atsR*::pDA27; Tp^r: Non-functional T6SS in a T6SS over-expressing background	Aubert *et al.*, 2008
K56-2 Δ*atsR*	K56-2 Δ*atsR*: Over-expresses the T6SS	Laboratory stock
K56-2 Δ*hcp* Δ*atsR*	K56-2 Δ*hcp* Δ*atsR*: Non-functional T6SS in a T6SS over-expressing background	Laboratory stock
KEM1	K56-2 *mgtC*::pKM3; Tp^r: Cannot delay phagosome maturation	Maloney and Valvano, 2006
E. coli strains		
DH5α	F- Φd*lacZ*Δ*M15* Δ(*lacZYA-argF*)*U169 endA1 recA1 hsdR*17 (r_K^- m_K^+) *supE44 thi-1* Δ*gyrA96 relAl*	Laboratory stock
Plasmids		
pHcp	pDA12; 0.5-kbp fragment encoding Hcp	Aubert *et al.*, 2008
pCmRed4	Derivative of pJRL1; additional *dhfr* promoter driving mRFP, Cm^r	Laboratory stock
pDA27	pGPΩTp; 272-bp internal fragment from *atsR*	Aubert *et al.*, 2008
pDA12	Cloning vector; ori_{pBBR1}, Tet^r, mob^+, P_{dhfr}	Aubert *et al.*, 2008
pGPΩTp	ori_{R6K}, ΩTp^r cassette, mob^+	Flannagan *et al.*, 2008
pKM3	pGPΩTp; 299-bp *mgtC* mutagenesis fragment	Maloney and Valvano, 2006

Tp^r, trimethoprim resistance; Cm^r, chloramphenicol resistance; Tet^r, tetracycline resistance; BCRRC, *B. cepacia* Research and Referral Repository for Canadian CF Clinics

spectrophotometer cuvette which already contained 0.9-millilitres of DMEM with 10% FBS, to produce a one-tenth dilution. The optical density (OD) of the dilution was recorded using a spectrophotometer and the value extrapolated to undiluted culture. Eukaryotic cells were seeded in six-well plates at a density of 0.5×10^6 cells per well. When cells were prepared for microscopy, a pyrogen-free cover-slip was placed in each well. For all other experiments, no cover-slip was added. Macrophages were estimated to have a doubling-time of approximately 15 hours and epithelial cells approximately 24 hours. Following the respective doubling time, each well had its media removed and was rinsed with PBS pre-warmed to 37°C. A volume of DMEM with 10% FBS was added to each well after the PBS rinse. Bacterial cells were then added to each well at the appropriate multiplicity of infection (MOI) for the respective experiment. Six-well plates were then centrifuged at 300 x g for one minute to synchronize the interaction of bacterial cells with eukaryotic cells throughout each sample. Plates were then placed in 37°C and 5.0% CO_2 conditions for the duration of each infection experiment. The same protocol was used to prepare samples for microscopy or flow cytometry.

Ac-DMQD-CHO was added to fresh DMEM with 10% FBS one-hour prior to infection. Cells were then incubated under standard growth conditions for one hour and rinsed three times with PBS prior to infection in fresh DMEM with 10% FBS.

2.6 – Opsonization and use of latex beads

Fluoresbrite YG microspheres with a 0.1 μm diameter (i.e. latex beads)(Polysciences Inc., Warrington USA) were incubated for one hour in PBS

supplemented with human IgG (Sigma-Aldrich Inc.) at 37°C. Beads were then centrifuged at 1500 x g, and rinsed with prewarmed PBS. This process was repeated three times. Beads were then resuspended in 2 mL of DMEM supplemented with 10% FBS and then plated onto macrophages at a ratio of 50 beads per one macrophage. Samples were then centrifuged at 200 x g for one minute, and placed into a tissue culture incubator running under standard conditions for the duration of the experiment.

2.7 - Immunostaining

Unless otherwise stated, incubations during the following protocol were conducted at room temperature in the absence of light. At the appropriate time post-infection, the growth medium was aspirated from six-well plates, and cells were rinsed three times with pre-warmed PBS. Four percent paraformaldehyde (v/v) was added to each well, and incubated for 30 min at room temperature, followed by three consecutive rinses with PBS. To quench reactive aldehyde products left over from paraformaldehyde fixation, 100 mM glycine solubilized in PBS was added and left to incubate for ten minutes, followed by three consecutive rinses with PBS. Cells were permeabilized to facilitate entry of antibodies into the cytoplasm, and this was conducted by adding 0.1% triton X-100 (v/v) solubilized in PBS supplemented with 5% powdered milk (w/v), and this solution was incubated for a minimum of one hour. The powdered milk in this solution was incorporated to act as a blocking reagent to improve the signal-to-noise ratio of fluorescence.

Following permeabilization, coverslips were placed on to a 100μL aliquot droplet of primary antibody diluted in 5% milk solution in PBS. Cells were incubated

with primary antibody for one hour, followed by three consecutive rinses with PBS. The process was repeated for the incubation with secondary antibodies. When required, one unit of Alexa Fluor 488 phalloidin was added during the secondary antibody incubation.

Following incubation with respective antibodies, coverslips were rinsed three times in PBS. Coverslips were then placed onto aliquots of Dako mounting medium previously deposited on the surface of a glass microscope slide. Mounted coverslips were stored at room temperature in the dark.

2.8 - Epifluorescence and phase-contrast microscopy

Images were acquired using a Qimaging cooled charge-coupled device (CCD) camera mounted on a Zeiss Axioscope 2 microscope with either an X100/1.3 numerical aperture Plan-Neofluor phase-contrast objective or a X10/1.3 numerical aperture Plan-Neofluor phase-contrast objective. Excitation of fluorescent compounds was done using a 50-watt mercury arc lamp. Digital processing of images was conducted using Northen Eclipse 6.0 imaging analysis software. When necessary, Northern Eclipse software was utilized for semi-automated enumeration through the application of monochromatic pixel differentiation tools available with this software.

2.9 - Confocal microscopy and three-dimensional modeling

Images were obtained using a Zeiss LSM 510 META/ConfoCor2 laser scanning confocal microscope and a 100X oil immersion objective. Imaris three-

dimensional imaging software was utilized to generate three-dimensional contours of Z-stacked images as per software protocol (Bitplane, Zurich, Switzerland).

2.10 – Flow cytometry

Bacterial infection of eukaryotic cells was completed as described previously. Control cells that were treated with either 0.05% saponin detergent (v/v) or 1μg/mL actinomycin D were prepared at the same time that experimental samples were infected with *B. cenocepacia.* After retrieval of infected samples, supernatants were placed into separate conical tubes to eliminate dead and/or floating cells. Adherent cells were dislodged from the substrate using PBS-based enzyme-free dissociation buffer (Invitrogen, Carlsbad, USA). Dislodged cells were mixed with respective supernatants. Conical tubes were centrifuged at 400x g and pellets were rinsed with ice-cold PBS. The centrifugation step was repeated once. Pellets were resuspended with 100 μL 1X Annexin V binding buffer (diluted in ddH_2O from 5X solution; 50 mM HEPES, 700 mM NaCl, 12.5 mM $CaCl_2$, pH 7.4). Cell suspensions were incubated for 15 minutes in the dark with fluorescein-conjugated Annexin V and propidium iodide (Invitrogen, Carlsbad, USA), as per manufacturer's instructions. Cells were transferred to glass test tubes and total volume of binding buffer was topped up to 500 μL. Test tubes were placed on ice and samples were analyzed by flow cytometry within one hour.

Flow cytometry analyses were performed using a FACSCalibur (BD Biosciences), data acquisition was performed using CellQuest Pro software, and data analysis was performed using FlowJo software.

2.11 - Growth curve analysis

Overnight cultures of the appropriate strains were grown as described above. One ml aliquots from overnight cultures were centrifuged at 16,000x g and rinsed with pre-warmed PBS. The centrifugation and rinse processes were repeated twice. Optical densities were obtained as described previously, and innocula were added to wells of microplates designed specifically for bioscreen equipment. Bioscreen experimentation was conducted at 37°C with constant shaking for thirty hours.

Media used for the bioscreen experiments included LB, DMEM alone, DMEM with 10% FBS, and DMEM with 10% FBS obtained from two-day old macrophage culture. This last medium was obtained during standard sub-culture of ANA-1 macrophages and then filter-sterilized using a filter with 0.22 μm pores.

2.12 - Statistical analyses

Unless otherwise stated, all relevant data was analyzed statistically via One-Way ANOVA with Tukey's post-test.

Chapter 3

Results

3.1 - Characterization of the T6SS-mediated protrusion phenotype

B. cenocepacia can induce the formation of actin-rich membrane protrusions in infected macrophages, and this phenomenon is mediated by a functional T6SS (Aubert *et al.,* 2008). Actin is critical to a number of host cell functions, including fusion events between a developing phagosome and the endosomal pathway (Kjeken *et al.,* 2004) and cell shape and mobility (Koestler *et al.,* 2008). The ability of this pathogen to subvert the host actin cytoskeleton could be related to the phagosome maturation delay induced within infected macrophages (Lamothe *et al.,* 2007). Therefore, the first component of this study was the characterization of the actin-rich irregular membrane protrusions induced by the T6SS of *B. cenocepacia* and the role of the T6SS in the phagosome maturation delay. To characterize the actin-rich protrusions it was crucial to determine: 1) the rate of protrusion formation post-infection, 2) the physical characteristics of the protrusions, and 3) whether the phenotype is connected to the delay in phagosome maturation.

3.1.1 - Kinetics of the actin-rich protrusion formation in ANA-1 macrophages

ANA-1 macrophages were used in this study because of previous observations in the laboratory that these cells display a robust protrusion phenotype in a T6SS-dependent manner (Aubert *et al,* 2008). To assess the dynamics of the T6SS-mediated protrusion formation in ANA-1 macrophages, we investigated whether there is a relationship between the number of internalized bacteria and the formation of membrane protrusions. ANA-1 macrophages were infected at an MOI of 50 for 1, 2, 4, and 6 hours with *B. cenocepacia* strains K56-2

wild-type and K56-2 *atsR*::pDA27 expressing RFP encoded by pCmRed4. Samples were fixed with paraformaldehyde and examined by epifluorescence microscopy. The following parameters were evaluated per field of view: total number of macrophages, number of macrophages containing internalized bacteria, number of macrophages demonstrating a protrusion-like phenotype, and the number of macrophages having internalized bacteria and also demonstrating protrusions. Although 46 ± 2% and 53 ± 4% of macrophages infected with K56-2 wild-type and K56-2 *atsR*::pDA27, respectively, displayed irregular membrane protrusions by 6 h post infection, there was a marked delay in protrusion formation by macrophages infected with wild-type at 1, 2 and 4 h post infection, compared to those infected with the *atsR*::pDA27 mutant strain. In contrast, 60 ± 2.5 % of ANA-1 macrophages infected with the atsR::pDA27 mutant displayed membrane protrusions at 2 hours post-infection. Given that protrusions formed predominantly in cells that contained internalized bacteria, there appears to be a correlation between number of internalized bacteria and the incidence of protrusions (Figure 5). These data suggest that the formation of protrusions is connected with bacterial internalization, and that the overexpression of the T6SS in the *atsR*::pDA27 mutant results in a more rapid appearance of protrusions. The lack of differences in the number of protrusions between macrophages engulfing wild-type and *atsR*::pDA27 mutant bacteria at 6 hours post-infection suggests that the T6SS is fully expressed by wild-type bacteria at this time point. Given that AtsR is a response regulator hybrid that normally represses T6SS, similar to RetS of *P. aeruginosa*, the

Figure 5: Kinetics of formation of T6SS-mediated actin-rich protrusions in ANA-1 macrophages. ANA-1 macrophages were infected with either red fluorescent K56-2 wild-type or K56-2 *atsR*::pDA27 at an MOI of 50, for 1, 2, 4, and 6 hours. Samples were fixed via paraformaldehyde and enumerated via epifluorescence microscopy. Samples were counted over 21 fields of view. Each field of view was enumerated for the total number of cells, the number of cells containing internalized bacteria, the number of cells demonstrating a protrusion-like structure, and the number of cells having internalized bacteria and also demonstrated a protrusion. The protrusion phenotype appeared to positively correlate with the presence of internalized bacteria. The K56-2 parental strain (wild-type) induced the formation of protrusions at 6 hours (A), while the K56-2 *atsR*::pDA27 mutant strain induced the formation of protrusions as early as 2 hours post-infection (B). Graphs represent data obtained from one or two independent experiments, depending on the time point. Graph indicates the presence of bacteria ("Bac" as in the legend) in conjunction with the presence of membrane protrusions ("Prot" as in the legend).

A

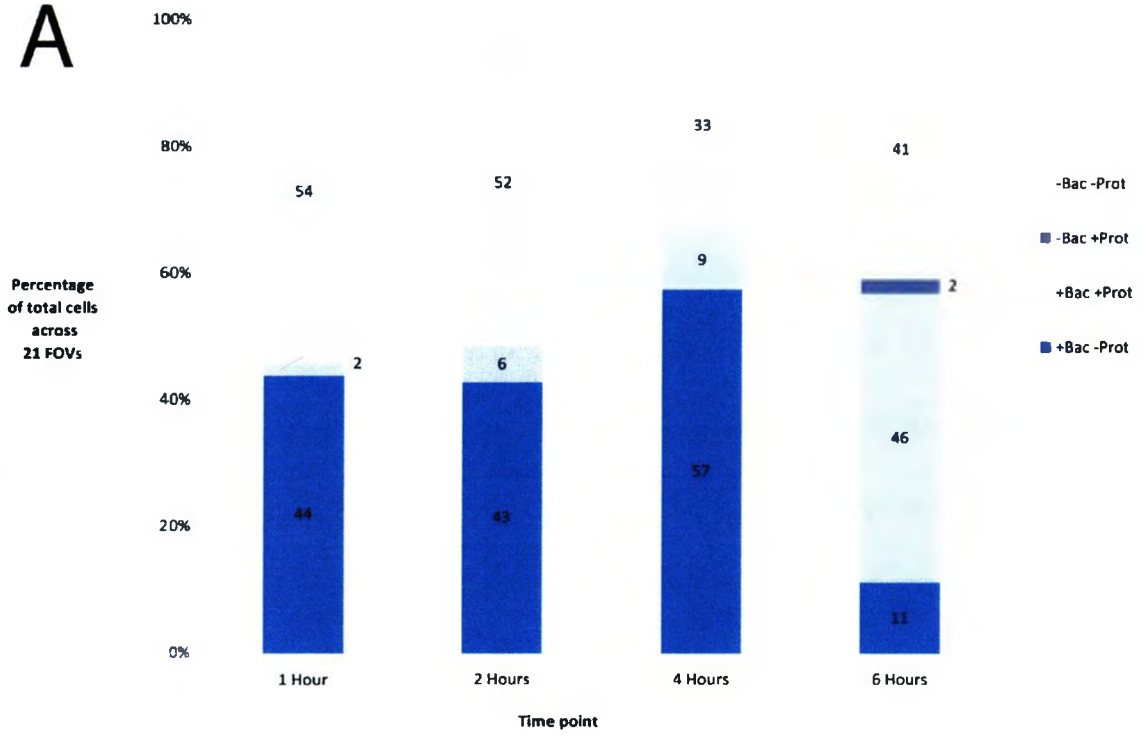
100%
80%
60%
40%
20%
0%
Percentage of total cells across 21 FOVs
54
52
33
41
2
6
9
2
44
43
57
46
11
1 Hour
2 Hours
4 Hours
6 Hours
Time point
-Bac -Prot
-Bac +Prot
+Bac +Prot
+Bac -Prot

B

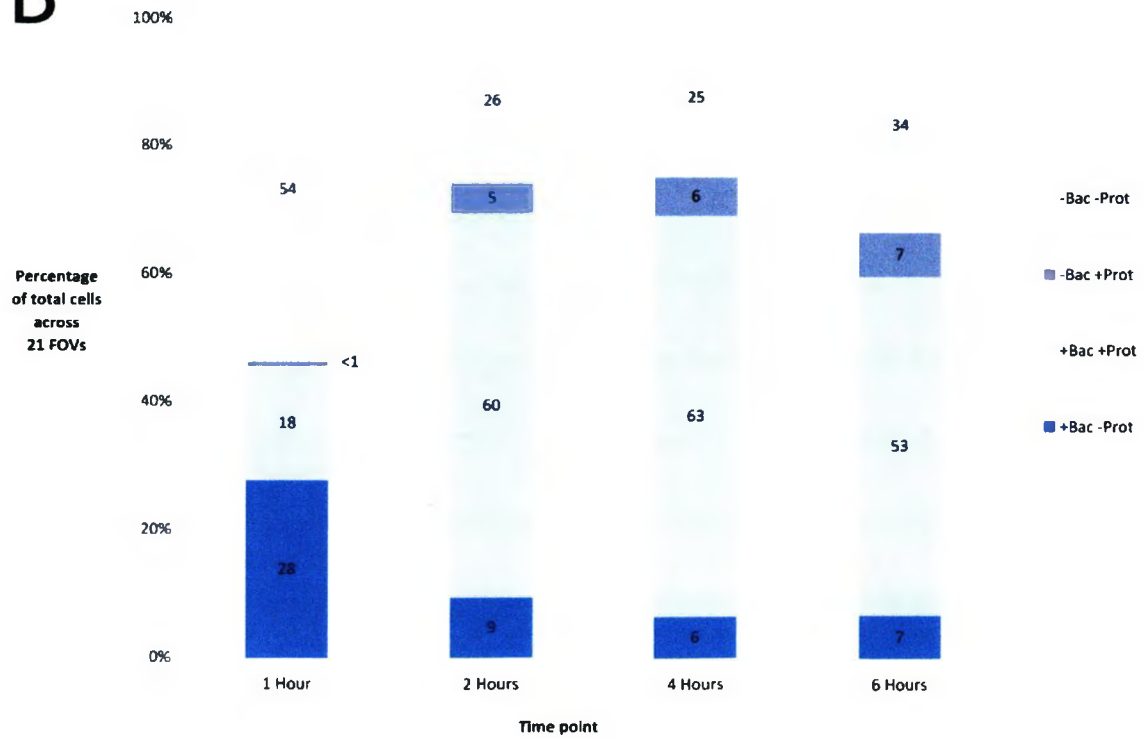
100%
80%
60%
40%
20%
0%
Percentage of total cells across 21 FOVs
54
26
25
34
<1
5
6
7
18
60
63
53
28
9
6
7
1 Hour
2 Hours
4 Hours
6 Hours
Time point
-Bac -Prot
-Bac +Prot
+Bac +Prot
+Bac -Prot

microenvironment within the maturing bacteria-containing vacuole could provide one or more signals that result in upregulated expression of T6SS components and in turn induction of host cell actin rearrangements.

3.1.2 - Presence of protrusions in A549 human lung epithelial cells

To determine if the T6SS phenotype was cell line- or mouse-specific, human-derived A549 human lung epithelial cells were infected with the K56-2 *atsR*::pDA27 strain. Infections were analyzed at various time points post-infection (1, 2, 4, 6 hours) and using various MOI (10, 50, 100, and 150 bacteria per eukaryotic cell). Human A549 cells generally have a broad, flat morphology, and grow together to form tissue-like clumps *in vitro* (Figure 6a). During infection with K56-2 *atsR*::pDA27, A549 cells demonstrated a rounded morphology and lattice-like membrane irregularities analogous to the membrane protrusions previously found with ANA-1 macrophages. The appearance of the lattice-like protrusions was only obvious and widespread within samples following at least 4 hours of infection and at a MOI of 100 or greater (Figure 6b). The higher MOI required could be due to poor phagocytic ability of A549 cells and previous observations of protrusion kinetics from this project suggest internalized bacteria and T6SS-mediated protrusion phenotypes may be correlated (Figure 5). From these data we conclude that the protrusion phenotype is not only a macrophage- or murine-specific phenomenon but can also take place in *B. cenocepacia*-infected human-derived epithelial cells.

Figure 6: Presence of the T6SS-mediated protrusions in A549 human epithelial cells. A549 epithelial cells were infected with the K56-2 *atsR*::pDA27 mutant strain at an MOI of 100 and the infection was allowed to proceed for 4 hours. Samples were fixed and visualized using phase-contrast microscopy. In an uninfected sample, cells are flattened broadly across the substrate without formation of protrusions (A). A phenotype similar to the actin-dense protrusion phenotype of macrophages was observed in infected A549 cells. The phenotype in epithelial cells resembled a lattice-like formation of opaque protrusions and a rounded morphology of the cell (B). White scale bars indicate 10 μm.

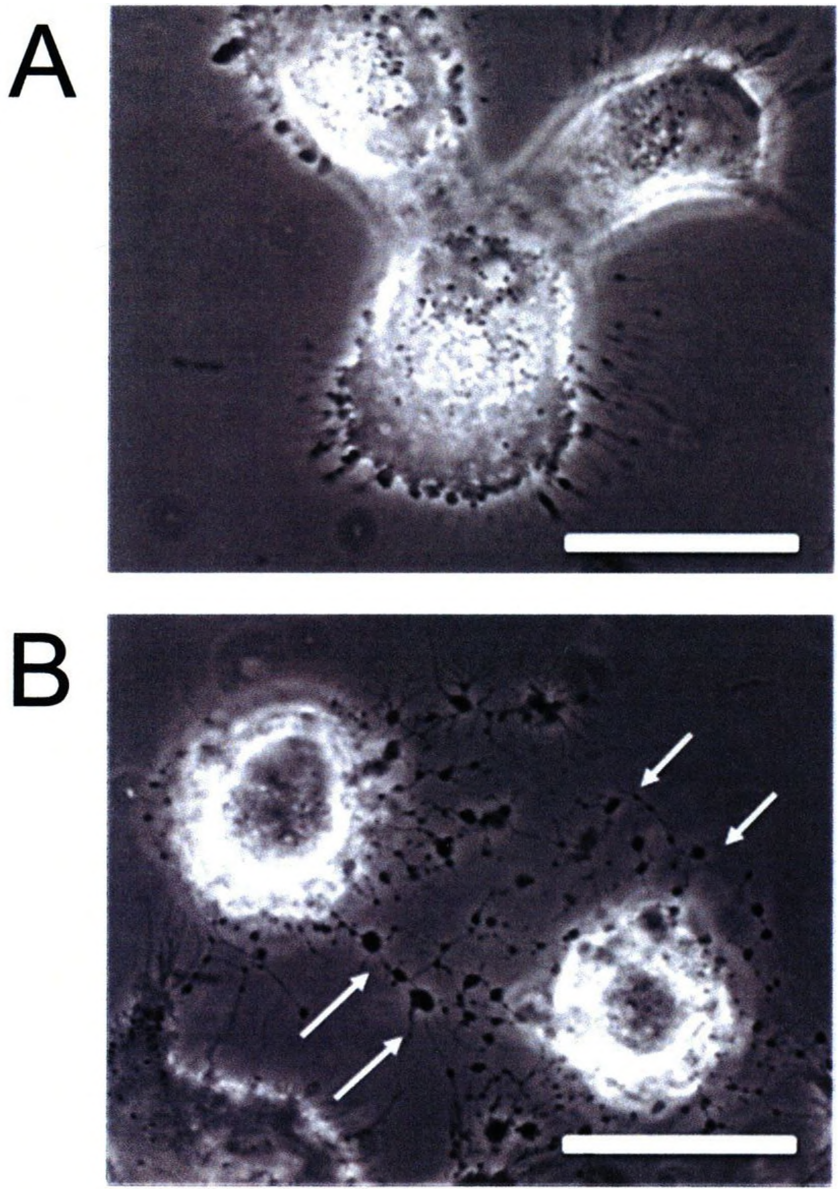
A
B

3.1.3 - Phagocytic index comparisons between ANA-1 and RAW 264.7 macrophages cell lines

The actin-rich protrusions are much less apparent during infections of RAW 264.7 macrophages (Aubert and Valvano, unpublished). This could be explained by differences in the phagocytic rate of RAW 264.7 macrophages compared to that of ANA-1 macrophages, especially if bacteria must be internalized to induce the protrusion phenotype. To determine if a difference in the rate of phagocytosis accounts for the discrepancy between these two cell lines, we performed phagocytosis experiments with either opsonized or non-opsonized latex beads. The opsonin used was polymeric human IgG, shown previously to be appropriate for use with murine macrophages (Marshall *et al.,* 2001). The proportion of cells that physically interacted with fluoresbrite latex beads differed significantly between ANA-1 and RAW 264.7 macrophages. The greatest difference can be seen between these cell types at the 4-hour time point, where 53.5 ± 14.6% and 73.6 ± 1.6% of ANA-1 macrophages associated with non-opsonized and opsonized latex beads, respectively. In contrast, less than 6.4 ± 4.5% of RAW 264.7 macrophages associated with non-opsonized latex beads ($p<0.01$), and approximately 36.3 ± 3.6% percent of these cells associated with opsonized beads ($p<0.01$). ANA-1 cells demonstrated greater affinity for latex beads than RAW 264.7, regardless of whether cells were enumerated for the incidence of at least one latex bead interacting with a macrophage (Figure 7a) or at least five latex beads interacting with cells (Figure 7b). These data also indicated that when RAW 264.7 cells were incubated with

Figure 7: Internalization of opsonized and non-opsonized latex beads by ANA-1 macrophages or RAW 264.7 macrophages. Macrophages were coincubated with either opsonized latex beads, or non-opsonized latex beads for one, two, or four hours. Samples were enumerated by counting the number of macrophages that bound or internalized at least one latex bead (A) or at least five latex beads (B). Data were obtained from 21 fields of view at 10X magnification using epifluorescence microscopy. Bar diagrams show the means and standard deviation of three independent experiments. Representative images of the samples stained with DAPI (pseudocoloured red) and auto-fluorescent latex beads (pseudocoloured yellow) from RAW 264.7 macrophages at four hours of co-incubation with non-opsonized latex beads (C) or opsonized latex beads (D). Representative images of the samples stained with DAPI (pseudocoloured red) and auto-fluorescent latex beads (pseudocoloured yellow) from ANA-1 macrophages at four hours of co-incubation with non-opsonized latex beads (E) or opsonized latex beads (F). White scale bars represent 100 μm.

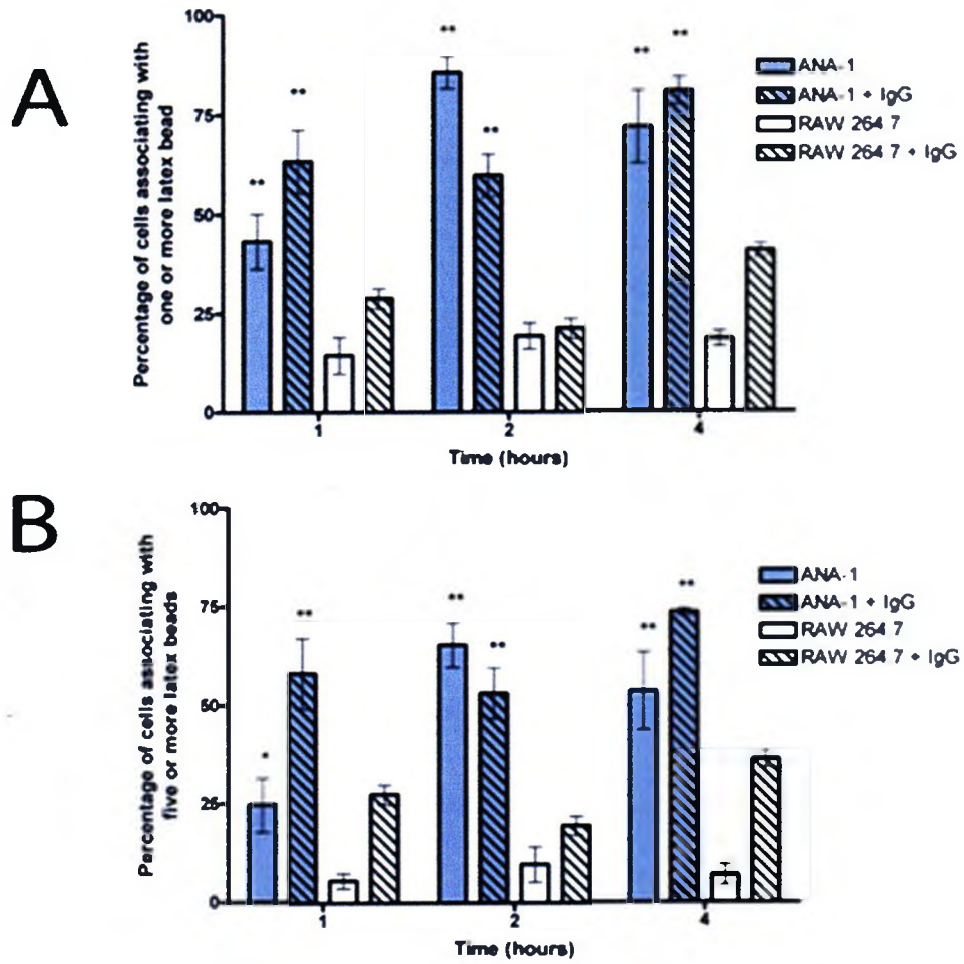
A
Percentage of cells associating with one or more latex bead
100
75
50
25
0
1
2
4
Time (hours)
ANA-1
ANA-1 + IgG
RAW 264.7
RAW 264.7 + IgG
B
Percentage of cells associating with five or more latex beads
100
75
50
25
0
1
2
4
Time (hours)
ANA-1
ANA-1 + IgG
RAW 264.7
RAW 264.7 + IgG

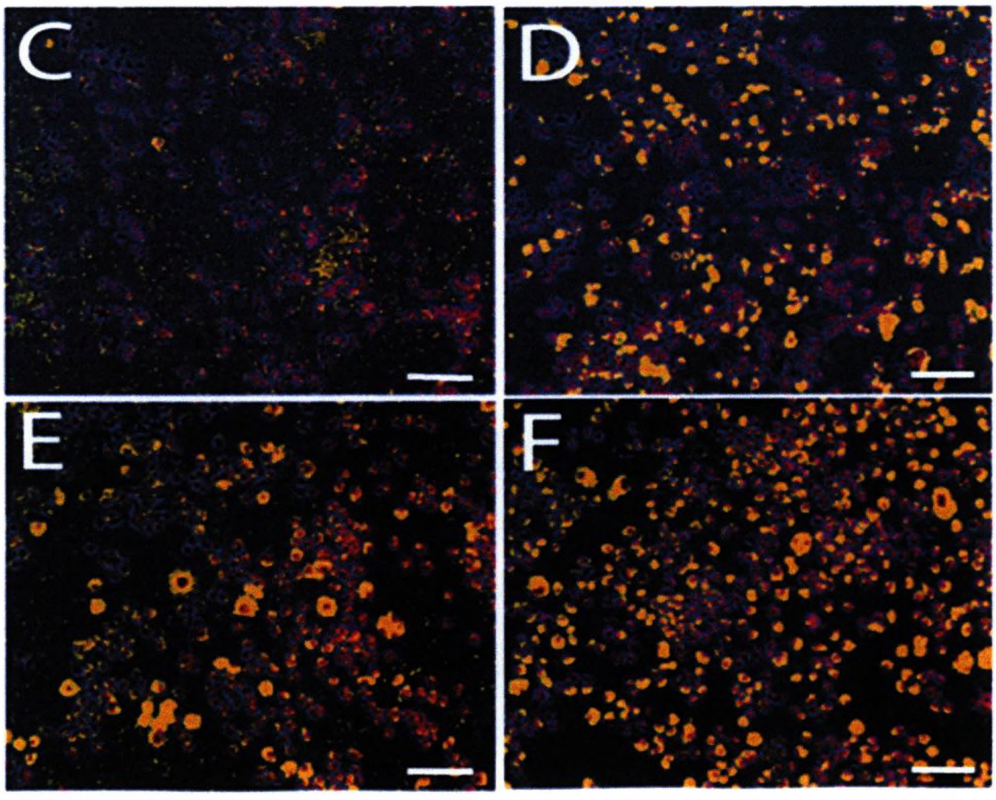
C
D
E
F

opsonized beads for four hours (36.3 ± 3.6%), association with beads had no significant difference to ANA-1 macrophages enumerated at one hour with non-opsonized beads (24.7 ± 11.3) ($p>0.05$). These data suggest that RAW 264.7 macrophages are less phagocytic than ANA-1 macrophages.

3.1.4 - Three-dimensional imaging of protrusions in ANA-1 cells

To better characterize the morphology of the actin-rich protrusions, confocal Z-stack imaging was conducted, followed by three-dimensional modeling of a contour over the stacked confocal images. As a result, the dynamic three-dimensional environment of long tubular projections between macrophages infected with K56-2 *atsR*::pDA27 was evaluated (Figure 8a). Certain physical observations could be made using the three-dimensional model. First, long tubular projections often had a branched appearance, with smaller, thinner projections radiating from thicker segments at acute angles (Figure 8b). Second, these thinner projections contacted the substrate while the thicker projection at their origin was seen to be slightly elevated above the surface (Figure 8c). Third, the phenotype is not limited to tubular projections along the surface of the substrate, but also results in irregular "spooling" of actin vertically above the substrate, which was not obvious from the top-down perspective of a standard microscope image (Figure 8d). We conclude from these data that the protrusions have a variety of morphological features that were not previously observed with other microscopy methods.

Figure 8: Three-dimensional modeling of the T6SS-mediated protrusion phenotype. ANA-1 macrophages were infected with K56-2 *atsR*::pDA27 at an MOI of 50 for 4 hours, at which point samples were stained with Alexa Fluor 488-conjugated phalloidin to visualize the actin cytoskeleton (green). Samples were imaged using confocal microscopy, and resultant Z-stacks were processed with Imaris image analysis software. A three dimensional contour was applied to Z-stack data, resulting in a three-dimensional model of an actin-dense protrusion between macrophages (A, centre). Inset images in B, C, and D relate the three-dimensional perspective relative to the overhead image (A). White arrows indicate points of interest. Rotation of the three dimensional model provided additional observations: the presence of polymerization of actin into irregular shapes in the vertical plane (B), the branching of actin-dense filaments at acute angles beneath primary protrusions (C), and the suspension of primary protrusions above the substrata supported by smaller filaments. Inset images in B, C, and D display perspective relative to A. White scale bars represent 10 μm in A, and 5 μm in C. Scale bars were not possible in B and D due to perspective.

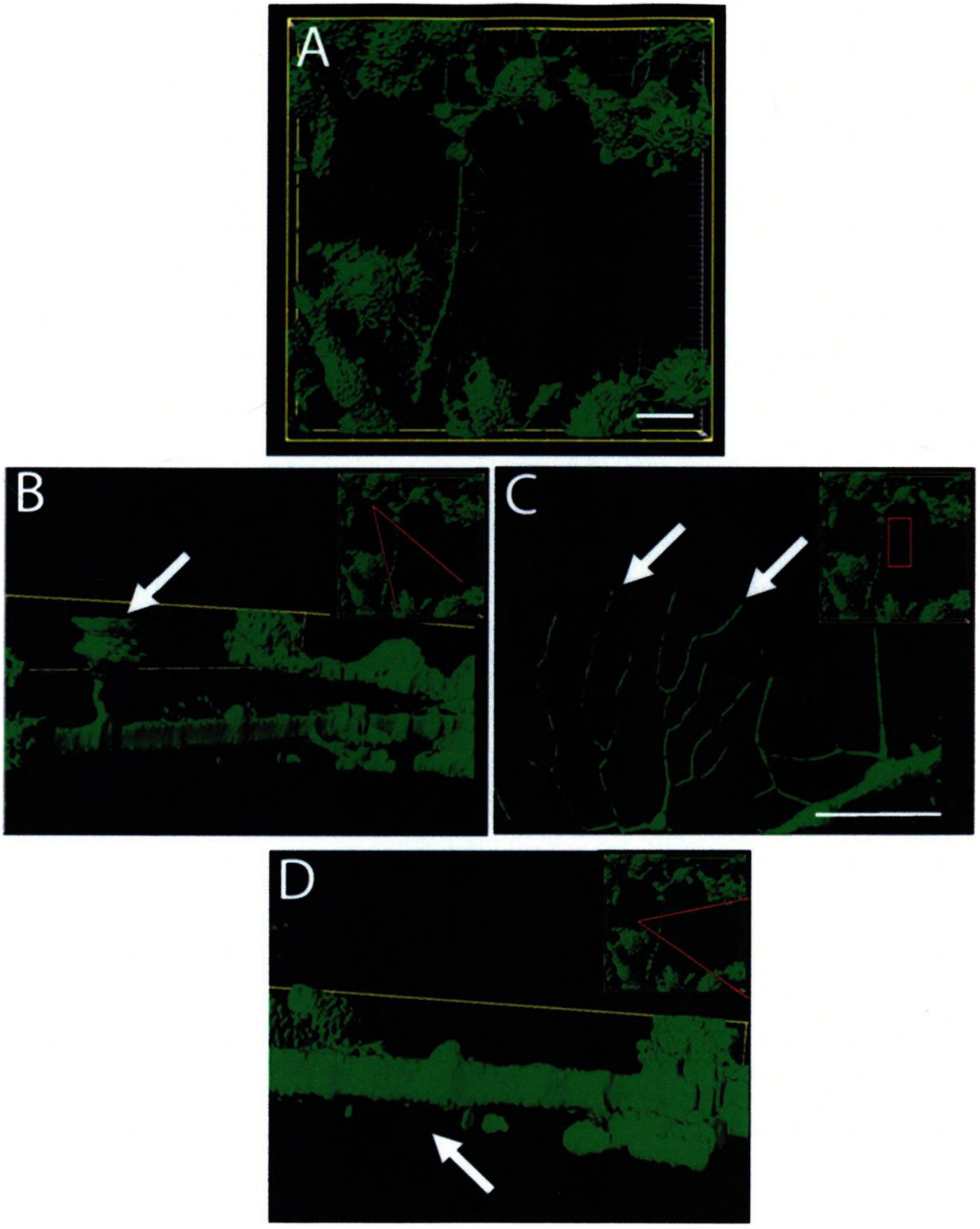
A
B
C
D

Using previously mentioned three-dimensional modeling techniques, it was noted that cells consistently demonstrated abnormal aggregation of actin away from the cell periphery when infected with K56-2 *atsR*::pDA27 for 4 hours at MOI 50. Using an antibody specific to formalin-fixed K56-2 membrane, it was found that these aggregations often appeared surrounded by an unknown protein, which bound the K56-2-specific antibody. In one particular case, this phenomenon was displayed prominently in four locations within an elongated macrophage (Figure 9a,b,c). Three-dimensional models were generated to demonstrate that the unknown protein surrounded actin, which was aggregated within the infected macrophage (Figure 9d,e,f). These data suggest that the modulation of host cell actin mediated by the T6SS may also involve other bacterial components other than the T6SS or that the antibody is cross-reactive with an unknown host protein.

3.1.5 - Effect of the T6SS on phagosomal LAMP-1 recruitment patterns

It was important to determine whether the apparent dysregulation of the actin cytoskeleton mediated by the T6SS played a role in the maturation delay previously shown in *B. cenocepacia*-containing vacuoles (BcCVs) (Lamothe *et al.*, 2007). Macrophages were infected with either K56-2 wild-type (pCmRed4), K56-2 *atsR*::pDA27(pCmRed4), or K56-2 Δ*hcp atsR*::pDA27(pCmRed4) at an MOI of 50 for 6, 8 or 10 hours. Macrophages were immunostained using rat anti-LAMP-1 and chicken anti-rat Alexa Fluor 488. Regardless of the infecting strain, the recruitment pattern of LAMP-1 to the BcCV membrane was sporadic and punctate around

Figure 9: Detection of an unknown protein associating with actin within ANA-1 macrophages infected with *B. cenocepacia*. Macrophages were infected with K56-2 *atsR*::pDA27 for 6 hours at MOI 50. Actin is shown in green and bacteria are red or pseudocoloured white, depending on figure shown. (A) A cluster of macrophages notably infected with bacteria (red) and one macrophage with an elongated appearance (centre). Actin appears surrounded by an unknown protein that bound the *B. cenocepacia*-specific antibody at three different locations (B, C; antibody represented in white). Bacteria stained with the antibody appear as hollow ovals (data not shown) which does not correspond to the shapes visualized in B, and C. Three-dimensional modeling of actin, using both semi-transparent modeling (D), and a solid contour (E) for the antibody revealed that the unknown protein appeared to surround actin. Additional instances could be found within this same cell (F) and in the majority of other cells within the sample (data not shown). White scale bar represents 10 μm. Dashed white box in A indicates area magnified in B, and C. White arrows in B and C indicates shape analyzed via three-dimensional model in D, and E.

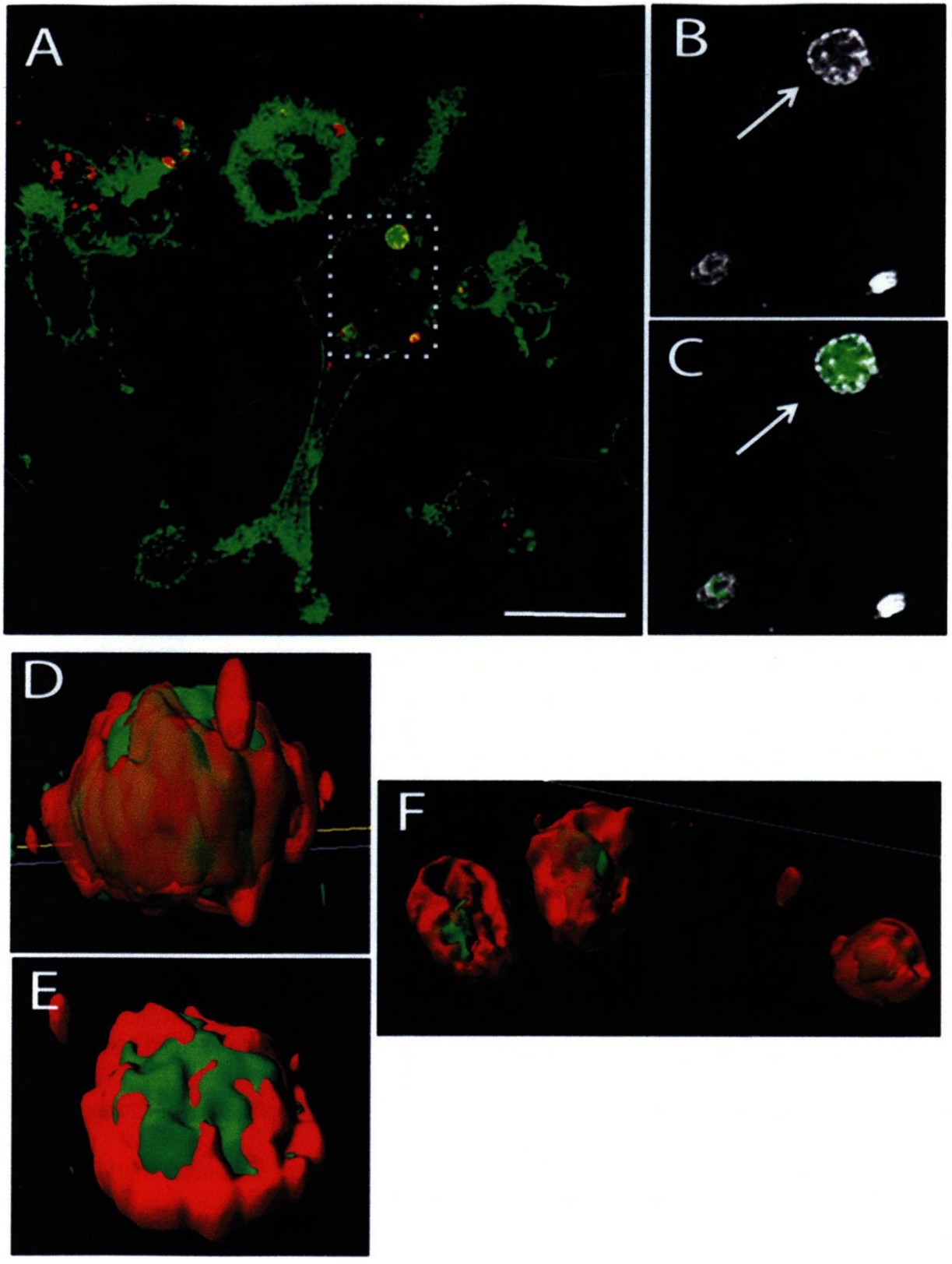
A
B
C
D
E
F

bacteria at the 6-hour time point (Figure 10a, top row of figures) and complete or ring-like at 10 hours post-infection (Figure 10a, bottom row of figures). Enumeration determined that there was no significant difference between any of the strains in terms of complete recruitment of LAMP-1 to the BcCV ($p>0.05$) (Figure 10b). At 6 hours post-infection macrophages infected with K56-2 Δ*hcp atsR*::pDA27(pCmRed4) displayed the greatest proportion of LAMP-1-positive BcCVs with 8 ± 0.7% and the smallest proportion of LAMP-1-positive BcCVs was displayed by those infected with K56-2 wild-type(pCmRed4) at 3.6 ± 1.1% ($p>0.05$). At 8 hours, the LAMP-1-positive BcCVs could be found in 54 ± 4.5% of macrophages infected with K56-2 wild-type(pCmRed4), and 40.6 ± 16.7% of those infected with K56-2 *atsR*::pDA27(pCmRed4) ($p>0.05$). At 10 hours, 81 ± 11% of macrophages infected with K56-2 Δ*hcp atsR*::pDA27(pCmRed4) had formed LAMP-1-rich BcCVs, while 74.7 ± 10.4% was displayed by cells infected with K56-2 *atsR*::pDA27(pCmRed4) ($p>0.05$). A positive control in the form of heat-inactivated K56-2 wild-type could not be produced because following heat inactivation, bacteria no longer fluoresced. Therefore, expression of a functional T6SS by *B. cenocepacia* is not required to delay the maturation of the host cell phagosome (Figure 10b). These data suggest that the phagosome maturation delay induced by *B. cenocepacia* is mediated by a virulence factor or factors other than the T6SS, and that the effect the T6SS has on host cell actin does not affect the maturation delay.

Figure 10: The T6SS of *B. cenocepacia* and LAMP-1 recruitment to BcCVs in ANA-1 macrophages. ANA-1 macrophages were infected at an MOI of 50 for 6, 8, and 10 hours with K56-2 wild-type, K56-2 *atsR*::pDA27, and K56-2 Δ*hcp atsR*::pDA27, each expressing red fluorescent protein via plasmid (pCmRed4). Samples were fixed and immunostained for LAMP-1 (green). Results indicated that regardless of the infecting strain, LAMP-1 recruitment followed a similar pattern of punctate fluorescence around bacteria at 6 hours, and complete ring formation by 10 hours post-infection (A). Samples were enumerated by counting the number of cells containing LAMP-1-rich compartments (ring-like pattern of fluorescence) with two or more red fluorescent bacteria. Data were gathered from 21 fields of view per sample, using three independent experiments. Results indicate quantitatively there is no observable difference between these strains in the recruitment of LAMP-1 to bacteria positive compartments, regardless of the functional status of the bacteria's T6SS. "NS" indicates no significant difference between bars that fall beneath the adjacent horizontal line. White Scale bar represents 10 μm.

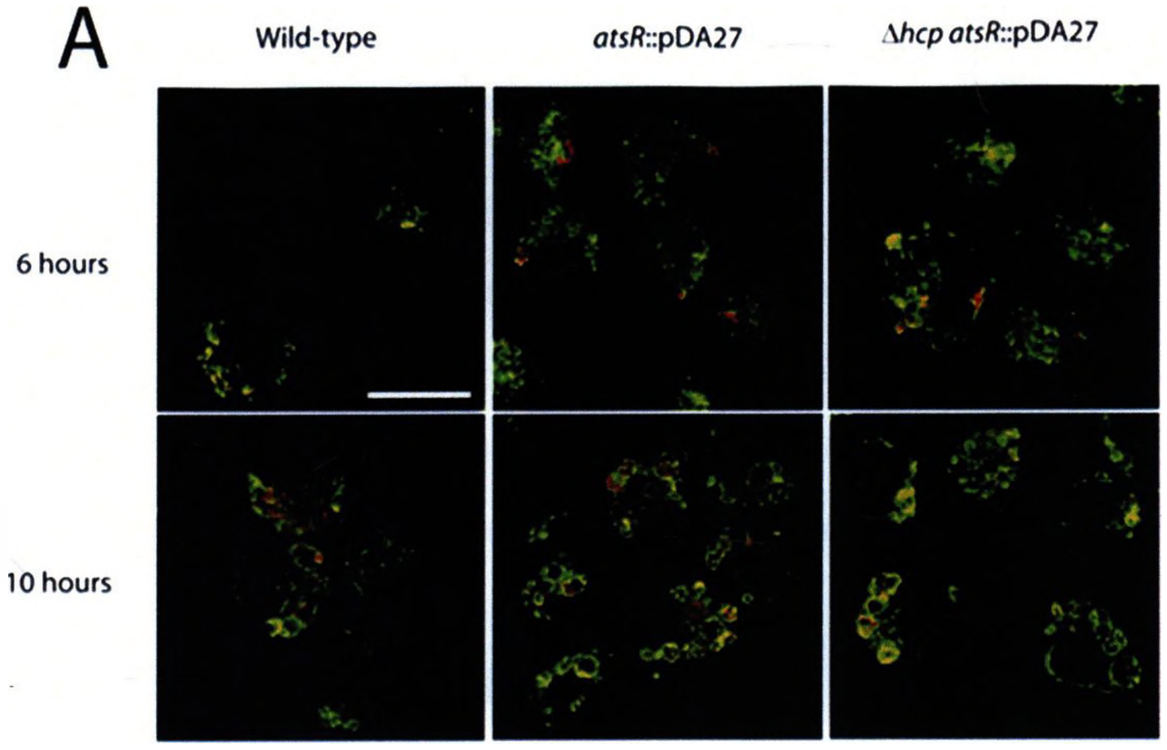
A
Wild-type
atsR::pDA27
Δhcp atsR::pDA27
6 hours
10 hours

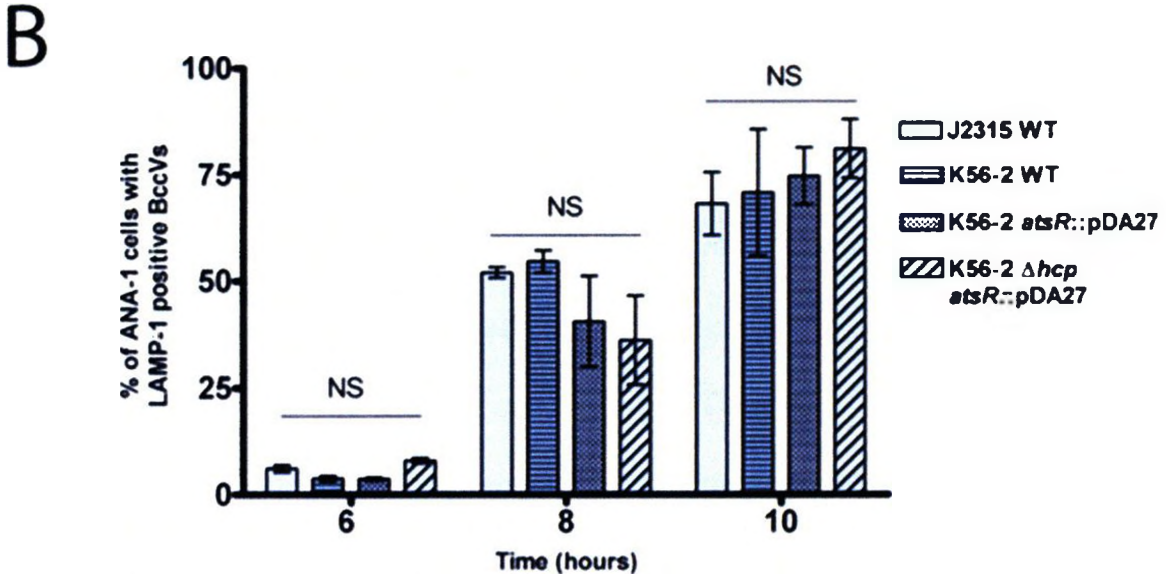
B
% of ANA-1 cells with LAMP-1 positive BccVs
100
75
50
25
0
NS
NS
NS
6
8
10
Time (hours)
J2315 WT
K56-2 WT
K56-2 atsR::pDA27
K56-2 Δhcp atsR::pDA27

3.2 - Characterization of the T6SS of *B. cenocepacia* in host cell death

During infection with K56-2 *atsR*::pDA27 cells appeared to undergo some form of cell death. Indeed, at 8 hours post-infection with K56-2 atsR::pDA27, DAPI-stained nuclear fragments are visible within membrane blebs while in an adjacent cell, bacteria can be seen exiting a LAMP-1 rich vacuole into the extracellular milieu (Figure 11a and b). These data suggest that the T6SS may be involved in the induction of some form of host cell death. Therefore, the second objective of this work was to determine whether T6SS mediates macrophage cell death.

3.2.1 - DAPI-based adherence and cytotoxicity assay

The presence of cell death required confirmation, and possible differences needed to be defined between K56-2 wild-type, K56-2 *atsR*::pDA27, and K56-2 Δ*hcp* *atsR*::pDA27. Under the assumption that a normally adherent ANA-1 macrophage will lose adherence during or following cell death, an assay was developed wherein macrophages infected for approximately 30 hours were fixed in paraformaldehyde, and stained with DAPI (Figure 12). Samples were then rinsed extensively with PBS to dislodge loosely adherent or dead macrophages. The residual DAPI-stained nuclei from each infection sample were then enumerated via microscopy. Using K56-2 wild-type, K56-2 *atsR*::pDA27, and K56-2 Δ*hcp* *atsR*::pDA27 strains, it was shown that samples of macrophages infected with K56-2 wild-type retained 95.8 ± 27.4 cells per FOV and those infected with K56-2 *atsR*::pDA27 retained 66.8 ± 30.8 cells per FOV. This is in contrast to samples of macrophages infected with K56-2 Δ*hcp*

Figure 11: Morphological evidence of cell death in ANA-1 macrophages infected with K56-2 *atsR*::pDA27. ANA-1 macrophages were infected with K56-2 *atsR*::pDA27 at an MOI of 50 for 8 hours. Samples were then fixed with paraformaldehyde, then immunostained for LAMP-1 (green) and stained with DAPI (blue). In the example image, the leftmost cell can be seen to undergo membrane blebbing (bottom two arrows) while the cell on the right appears to be equilibrating with the extracellular media, allowing intracellular bacteria to escape (top-right arrow) (A). Through a merge of blue and green fluorescence (B), it can be seen that membrane blebs contain DAPI-stained DNA , and that the vacuole previously containing K56-2 *atsR*::pDA27 stains positively for LAMP-1, suggesting those bacteria originally resided within that cell for the duration of phagosome maturation prior to escape into the extracellular media. White scale bars represent 5 μm.

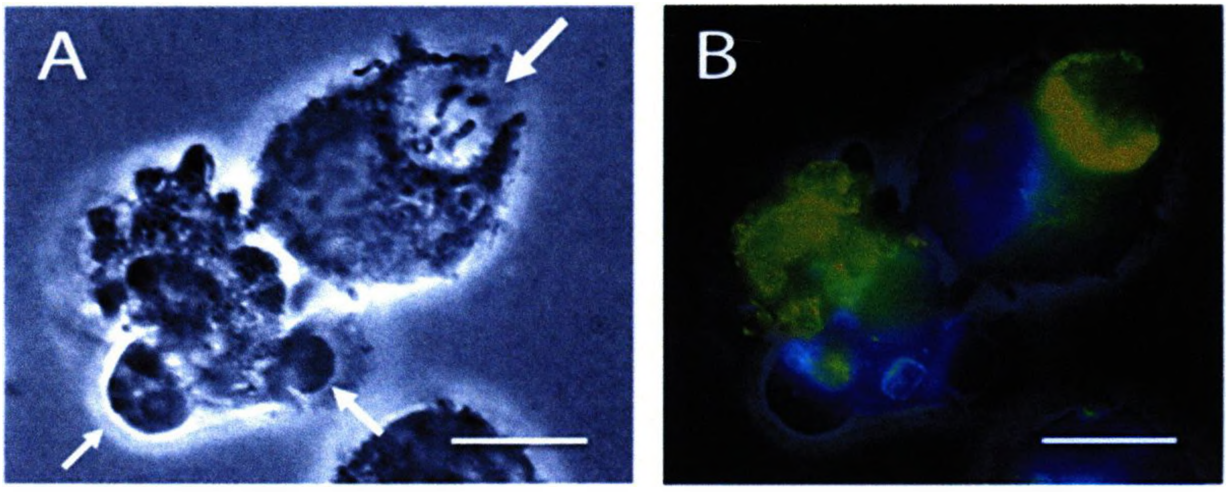
A
B

Figure 12: DAPI-based macrophage adherence assay following 30 hour infections. ANA-1 macrophages were infected with various strains (as indicated) with an initial MOI of 10 for 30 hours. Samples were then fixed and stained with DAPI. Cells were then enumerated with phase-contrast microscopy at 10X magnification. Residual macrophage nuclei were enumerated across 21 fields of view. K56-2 Δ*hcp* Δ*atsR* infection resulted in the greatest residual adherence among infected samples. Complementation of this phenotype through the reintroduction of *hcp* via plasmid (A). Data are representative of three independent experiments. Asterisks (***) indicate $p < 0.001$. Qualitative images representative of data found in A: (B) Uninfected control, (C) Heat-killed K56-2 WT control, (D) K56-2 WT, (E) K56-2 Δ*atsR*, and (F) K56-2 Δ*hcp* Δ*atsR*. Residual macrophages displayed morphological features suggesting cell death may be involved in loss-of-adherence as depicted by phase-contrast (G) and DAPI fluorescence (H) at 100x magnification (dashed circles indicate incidence of membrane blebbing and DAPI-stained DNA within blebs). Scale bars in B and D represent 100 μm, and scale bars in G and H represent 10 μm.

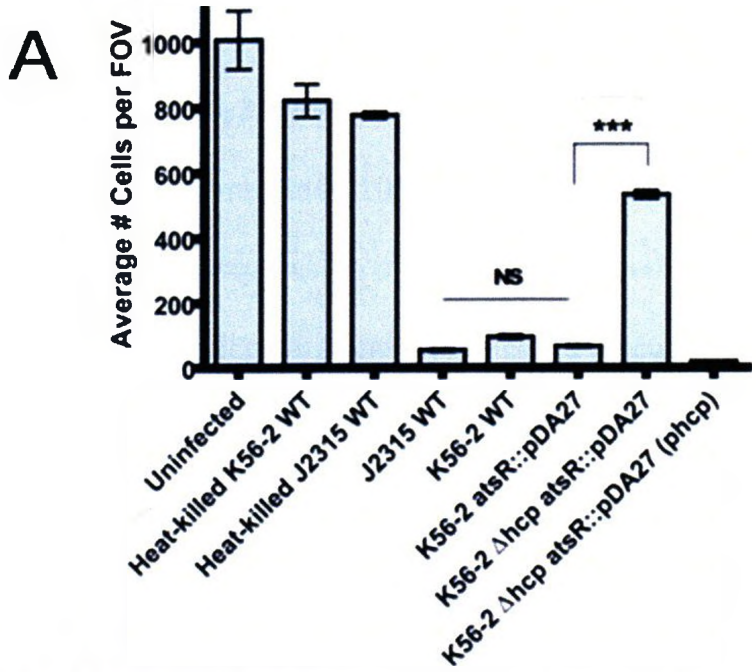
A
Average # Cells per FOV
1000
800
600
400
200
0
***
NS
Uninfected
Heat-killed K56-2 WT
Heat-killed J2315 WT
J2315 WT
K56-2 WT
K56-2 atsR::pDA27
K56-2 Δhcp atsR::pDA27
K56-2 Δhcp atsR::pDA27 (phcp)

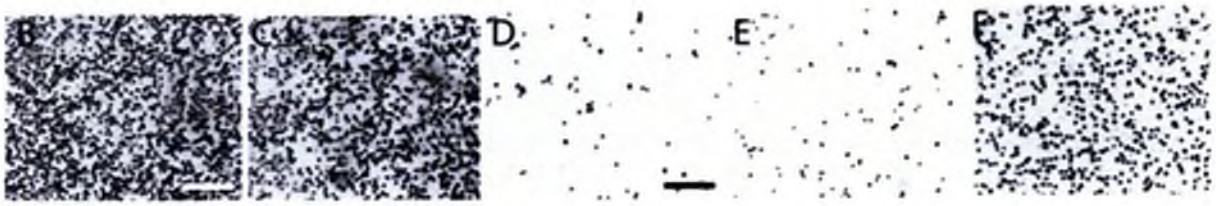
B
C
D
E
F

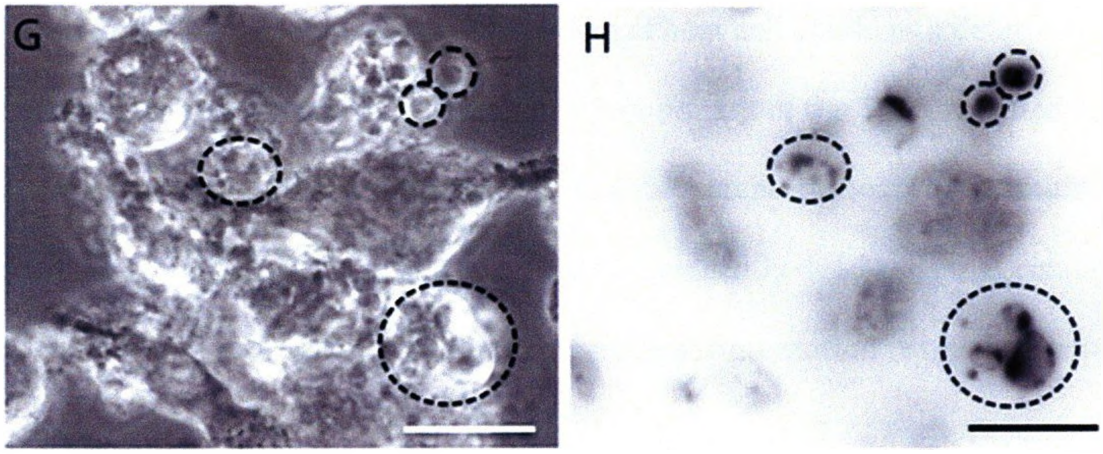
G
H

atsR::pDA27 that retained 533.3 ± 83.6 cells per FOV ($p<0.001$). Though this difference is quite large, K56-2 Δ*hcp atsR*::pDA27 was still significantly different from uninfected cells, which retained 1007.2 ± 70.3 cells per FOV ($p<0.001$)(Figure 13). Importantly, when the expression of Hcp was restored via plasmid in strain K56-2 Δ*hcp atsR*::pDA27 (pHcp) the phenotype could be complemented to 19.4 ± 1.9 cells per FOV. The possibility remained that live cells were dislodged following this protocol, or that cells in the early stages of cell death remained adherent. Furthermore, upon closer examination at 100x magnification, it was determined that a proportion of residual macrophages displayed cell death morphologies but without losing adherence in each sample. The morphological features observed included blebbing of the cell membrane and the appearance of DAPI-stained DNA within those blebs. These results indicate that the T6SS of *B. cenocepacia* may be involved in the induction of some mechanism of host cell death, as a deletion of the *hcp* gene, which encodes a major structural component of the T6SS, resulted in increased host cell viability, or reduced host detachment, compared to strains expressing a functional T6SS. The presence of apparently dead cells that retained adherence to the substrate required follow up experimentation using more specific reagents.

3.2.2 - Bicolour flow cytometry analysis using annexin V and propidium iodide

Flow cytometry analysis was conducted to more firmly establish that cell death is a consequence to host cells infected with T6SS-expressing strains of *B. cenocepacia*. Annexin V conjugated to a green fluorophore was used to determine

the degree of phosphatidylserine flipping to the outer leaflet of macrophage membranes, an indicator of apoptosis. The vital dye propidium iodide was used to differentiate cells that lost membrane integrity and became necrotic. Gating of samples was determined through the use of two positive controls. First, 0.5 μg/mL actinomycin D was employed as a chemical inducer of apoptosis, and second, 0.05% saponin detergent (w/v) was used to lyse macrophage membranes and, therefore, serve as a control for necrotic cell death. Through the use of these positive controls, quadrant gates were assigned around each of these two control populations, with the lower left quadrant indicating the proportion of cells that remained viable after experimental treatment or infection. These quadrant gates were then applied to experimental sample dotplots that were acquired from ANA-1 macrophages infected with K56-2 wild-type, K56-2 Δ*atsR,* K56-2 Δ*hcp,* K56-2 Δ*hcp* Δ*atsR,* and K56-2 *mgtC*::pKM3. The *mgtC* mutant, K56-2 *mgtC*::pKM3, was used to control for the growth of extracellular bacteria, as these bacteria grow normally but are compromised for survival once they are phagocytized (Maloney & Valvano, 2006).

It was determined that the majority of ANA-1 macrophages remained viable at 6 hours post-infection, regardless of the strain used to infect ($p>0.05$). However, at 12 and 24 hours, the incidence of some form of cell death increased dramatically amongst all live strain infections (Figures 13 and 14). Similar to the DAPI-based cytotoxicity assay, among infected samples the greatest host cell viability was found with the *atsR* and *hcp* double mutant, in this case, K56-2 Δ*hcp* Δ*atsR* strain, with 75.4 ± 6% viability at 12 hours ($p<0.001$) and 36.8 ± 13.6% viability at 24 hours ($p<0.05$), as compared to K56-2 wild-type with 52.5 ± 5.4% viability at 12 hours,

Figure 13: Percentage viability of ANA-1 macrophages following infection with K56-2 as assayed by bicolour flow cytometry analysis. ANA-1 macrophages infected for 6, 12, or 24 hours with various strains were assayed by flow cytometry. The proportion of cells which remained double-negative for annexin V and propidium iodide staining is indicated. ANA-1 macrophages infected with K56-2 Δ*hcp* Δ*atsR* displayed a strong significant difference at 12 hours ($p < 0.01$) and a slight significant difference at 24 hours ($p < 0.05$) in terms of viability compared to macrophages infected with all other strains. Data are representative of the means of three independent experiments.

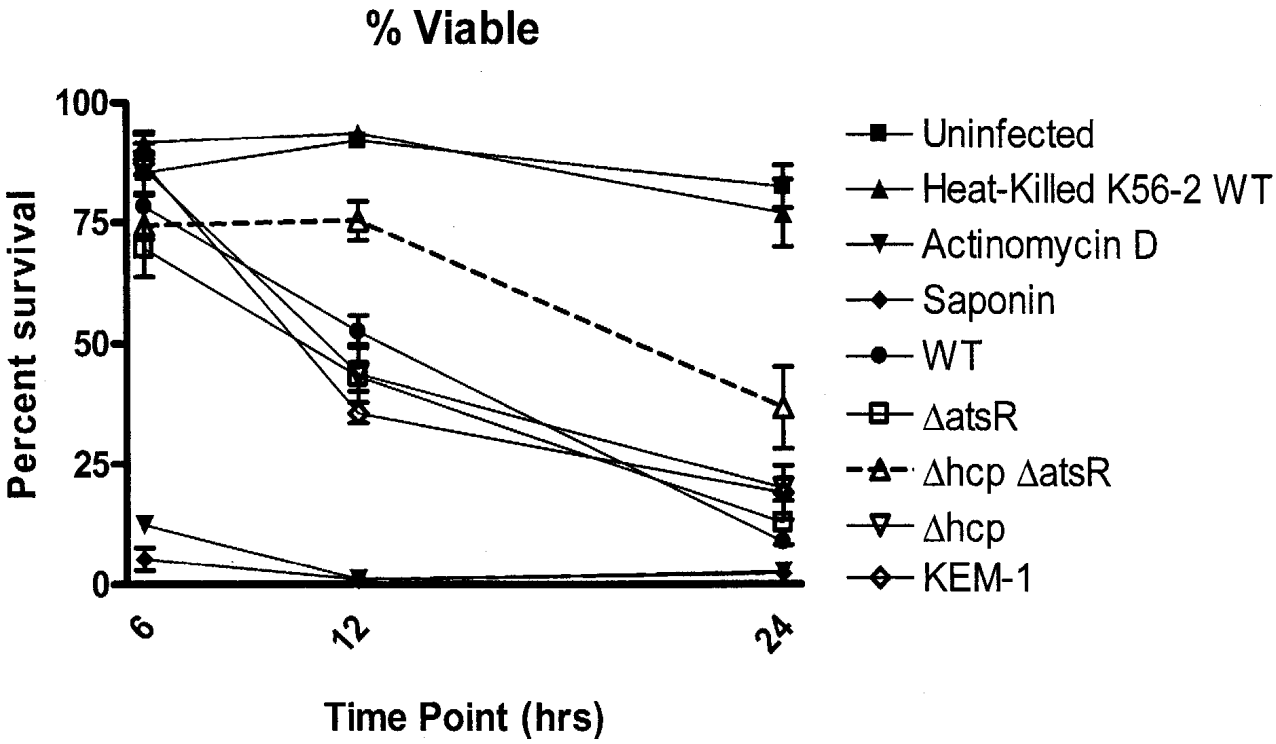
% Viable
Percent survival
100
75
50
25
0
6
12
24
Time Point (hrs)
Uninfected
Heat-Killed K56-2 WT
Actinomycin D
Saponin
WT
ΔatsR
Δhcp ΔatsR
Δhcp
KEM-1

Figure 14: Bicolour flow cytometry analysis data for double negative, annexin V-positive, and propidium iodide-positive populations. Data obtained following bicolour flow cytometry analysis of ANA-1 macrophages infected with indicated strains or treated with indicated control treatments. Macrophages were stained with annexin V and propidium iodide. Double-negative population from each treatment are indicated in the top row, annexin V-positive/propidium iodide-negative population from each treatment is indicated in the middle row of figures, and the double-positive and annexin V-negative/propidium iodide-positive populations are represented in the bottom row of figures. Data are representative of the means of three independent experiments. Asterisks (***) indicate $p < 0.001$ and (*) indicate $p < 0.05$.

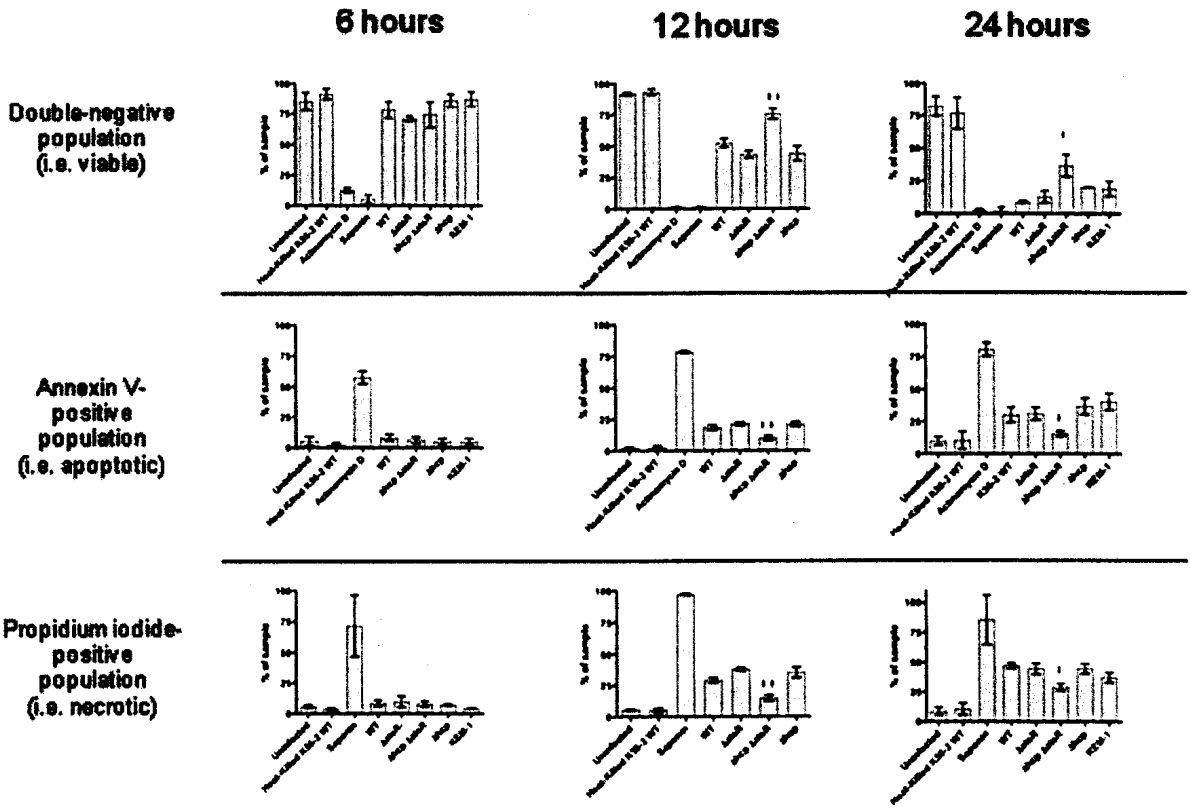
6 hours
12 hours
24 hours
Double-negative population (i.e. viable)
Annexin V-positive population (i.e. apoptotic)
Propidium iodide-positive population (i.e. necrotic)

and 8.9 ± 3.2% viability at 24 hours (Figure 14). Surprisingly, the K56-2 Δ*hcp* strain did not have a significant decrease in the induction of cell death when compared to K56-2 wild-type or K56-2 Δ*atsR,* despite the fact that K56-2 Δ*hcp* lacks a functional T6SS. It was not possible to discern between apoptosis and necrosis using the annexin V and propidium iodide bicolour staining (Figure 14, middle and bottom rows), though in either case, infections with K56-2 Δ*hcp* Δ*atsR* demonstrated the lowest incidence of any type of cell death. Also, the K56-2 *mgtC*::pKM3 strain was not compromised for the induction of host cell death, suggesting that either the induction of host cell death occurs shortly after phagocytosis before this strain can be degraded, or that this strain is not compromised for survival within a phagocytic cell.

These data confirmed that macrophages have greater viability when infected with a strain of K56-2 with both *atsR* and *hcp* deleted or disrupted than when infected with a strain of K56-2 with either of these genes intact. This corroborates data obtained with the DAPI-based adherence assay. However, these results complicated the issue because disruption of the T6SS through deletion of *hcp* alone was not sufficient to increase macrophage viability during infection.

3.2.3 - Confirmation of T6SS mutants used during flow cytometry study

Due to the unexpected result that the K56-2 Δ*hcp* strain, despite lacking a functional T6SS, induced cell death to a degree comparable to that of K56-2 wild-type or K56-2 Δ*atsR*, it was important to validate the genotypes of these strains following the flow cytometry analysis. Overnight cultures of these strains were used

to inoculate wells of a bioscreen plate, which contained one of four different media: LB broth, DMEM with no FBS, or DMEM supplemented with 10% FBS, or DMEM with 10% FBS obtained from macrophage culture and filter-sterilized (following potentially non-sterile conditions within a tissue culture incubator). The plate was incubated with gentle shaking for 30 hours. Following incubation, no significant growth differences were seen in any of the strains used for the flow cytometry study when grown in LB broth (Figure 15). However, none of the strains grew in any of the defined DMEM macrophage media types, despite that after 24 hours of co-incubation with macrophages, infected sample media becomes turbid without shaking. The presence of actin-rich irregular membrane protrusions was also reconfirmed, and correlated once again with the presence of a functional T6SS (Figure 16). These data suggest that *B. cenocepacia* cannot grow in defined DMEM media types without the presence of either macrophages or atmospheric growth conditions found within tissue culture incubators, such as 5% carbon dioxide. Furthermore, the absence of actin-rich protrusions in macrophages infected with either K56-2 Δ*hcp* or K56-2 Δ*hcp* Δ*atsR* indicates that the T6SS of both of these strains is non-functional, despite the wild-type levels of macrophage cell death following infection with K56-2 Δ*hcp*.

3.2.4 - T6SS-mediated cell death may not be caspase-3-dependent

To evaluate if caspase-3 was responsible for the annexin V-positive macrophage population a caspase-3 specific inhibitor, Ac-DMQD-CHO, was used.

Figure 15: Growth curve analysis of *B. cenocepacia* K56-2 wild-type and mutants grown in four different media types. Bacterial strains were grown overnight in LB broth, and sample of each was used to inoculate wells of a bioscreen plate using different media types. Media included LB, DMEM without FBS, DMEM supplemented with 10% FBS, and DMEM with 10% FBS which was filter-sterilized after being obtained from macrophage culture following two days of incubation.

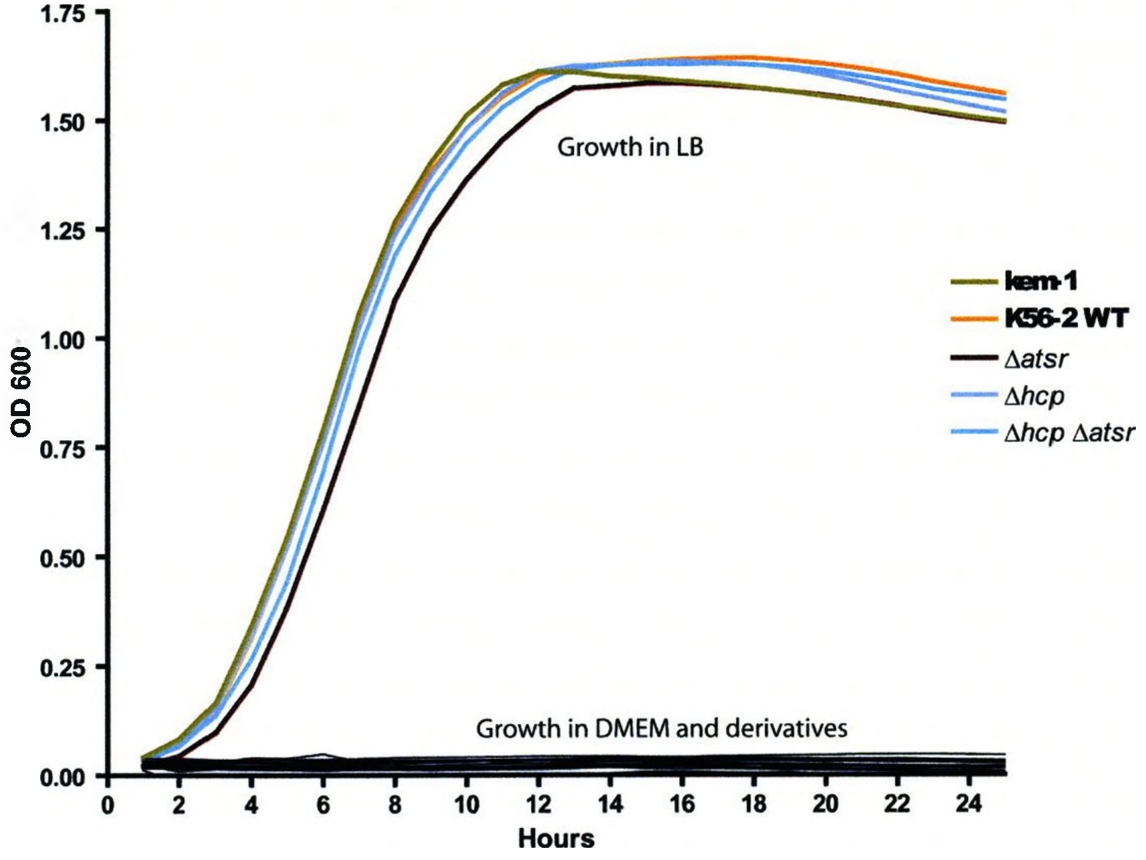
1.75
1.50
1.25
1.00
0.75
0.50
0.25
0.00
OD 600
0
2
4
6
8
10
12
14
16
18
20
22
24
Hours
Growth in LB
Growth in DMEM and derivatives
kem-1
K56-2 WT
Δatsr
Δhcp
Δhcp Δatsr

Figure 16: Microscopy confirmation of T6SS-mediated phenotype induced by strains used for flow cytometry. ANA-1 macrophages were infected with respective strains of K56-2 for 6 hours at MOI 50. Samples were then observed under 100X magnification by phase-contrast microscopy to confirm the presence of the protrusion phenotype following macrophage infection using strains that expressed a functional T6SS. (A) uninfected cells display a rounded morphology characteristic of healthy ANA-1 macrophages, (B) K56-2 WT and (C) K56-2 Δ*atsR* bacteria induce the formation of protrusions, as previously observed, and neither (D) K56-2 Δ*hcp* nor (E) K56-2 Δ*hcp* Δ*atsR* can induce the formation of protrusions. (F) KEM-1 (*mgtC*::pKM3) bacteria induce the formation of protrusions despite reportedly being incapable of prolonged intraphagosomal survival. Arrows indicate the location of protrusions. Scale bar represents 10 μm.

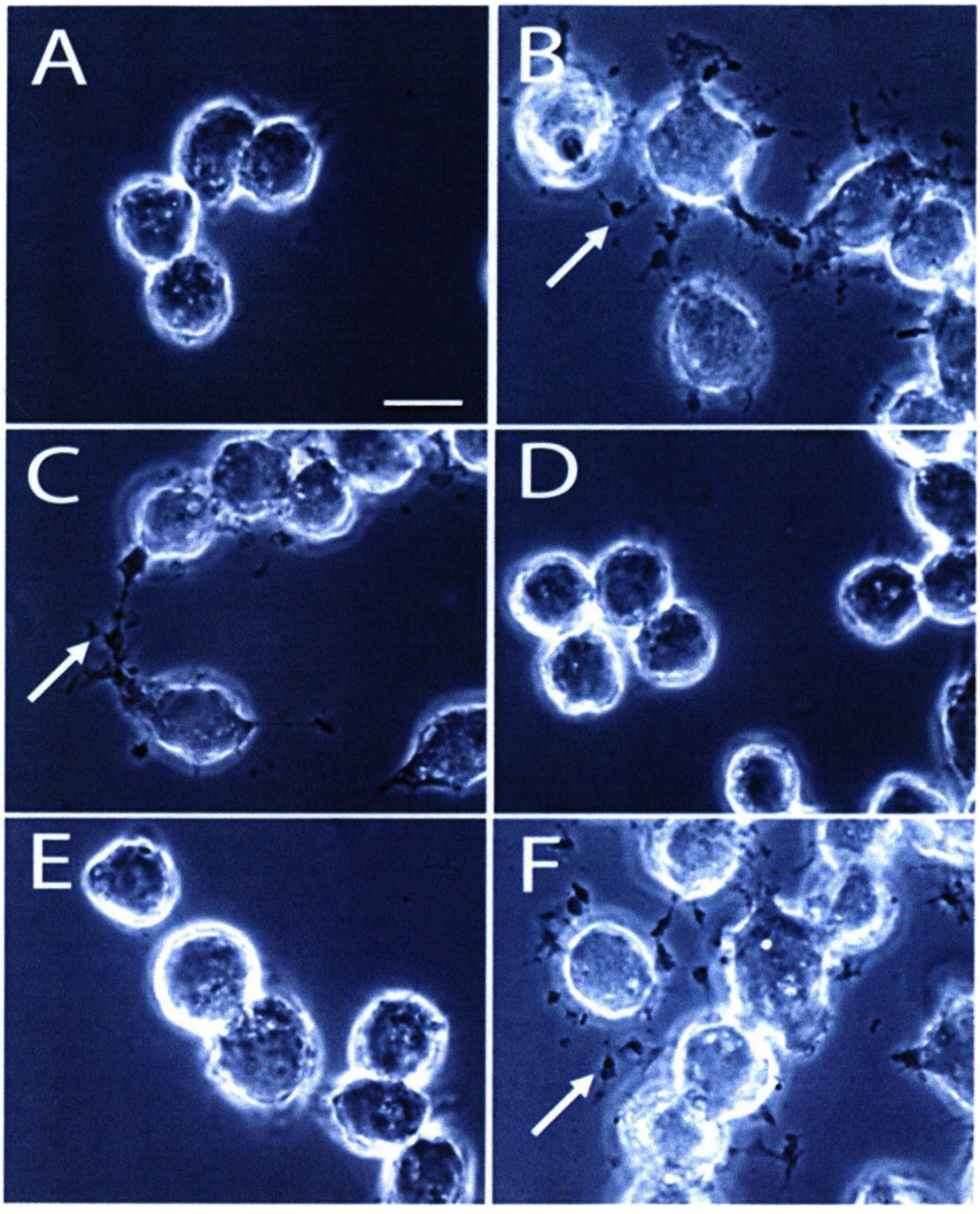
A
B
C
D
E
F

Cells were pre-incubated for one hour prior to infection with K56-2 wild-type. Results indicated that common concentrations for the caspase-3 inhibitor did not increase viability of macrophages during 24-hour infection with K56-2 wild-type bacteria (Figure 17). These data suggest that the mechanism of cell death induced by *B. cenocepacia* may not be solely caspase-3-dependent apoptosis or that the Ac-DMQD-CHO caspase-3 inhibitor could not sufficiently inhibit caspase-3 to prevent the induction of cell death.

Figure 17: ANA-1 macrophage cell death and the role of caspase-3. ANA-1 macrophages were pre-incubated for one hour with 20 μM or 50 μM concentrations of Ac-DMQD-CHO. Samples were then rinsed and infected with MOI 10 of K56-2 WT. Infections were allowed to progress for 24 hours, at which point they were processed for bicolour flow cytometry using annexin V and propidium iodide. Control and experimental samples are represented proportional to 100% uninfected control; actual viable cell population of the uninfected sample was approximately 95%. Samples treated with inhibitor showed no significant difference in the amount of annexin V-negative, propidium iodide-negative (i.e. viable) macrophages as compared to the untreated K56-2 WT sample. DMSO serves as vehicle control for Ac-DMQD-CHO. Data represent means of three independent experiments. "NS" indicates no significant difference between bars underneath adjacent horizontal line.

% annexin V-negative,
propidium iodide-negative
compared to control
0
25
50
75
100
Control
DMSO (Vehicle)
20 uM Caspase-3 Inhibitor
Actinomycin D
K86-2 WT
WT + 20uM Caspase-3 Inhibitor
WT + 50uM Caspase-3 Inhibitor
NS
SN

Chapter 4

Discussion

4.1 - Characterization of the actin-rich protrusion phenotype in macrophages infected with *B. cenocepacia*

In this study, we examined the actin-rich membrane protrusions induced in macrophages by the T6SS of *B. cenocepacia.* It was found that K56-2 wild-type induced protrusions at 6 hours post-infection, while the K56-2 *atsR*::pDA27 mutant induced protrusions earlier at 2 hours post-infection. This suggests that one or more stimuli within the bacteria-containing vacuole may account for the activation of the T6SS. It has been shown by a luciferase expression assay that T6SS may be pH regulated, such that at pH 5, expression of T6SS components reaches a peak level (Aubert and Valvano, unpublished). However, at the present time the signal involved in expressing T6SS *in vivo* remains unknown.

We also determined that the presence of protrusions appeared related to internalization. Another macrophage cell line, RAW 264.7, was less able to engulf beads than ANA-1 macrophages (Figure 6) and would also only rarely produce protrusions during K56-2 *atsR*::pDA27 infection (data not shown). It is difficult to extrapolate the phagocytosis of inert latex beads with phagocytosis of live bacteria that are capable of inducing a phenotype. However, these observations may provide a partial explanation for the differences noted between protrusion phenotypes seen in both RAW 264.7 and ANA-1 macrophages. In macrophages, thick protrusions remain above the substrate and radiate smaller protrusions at acute angles that contact the substrate. This is similar to the patterned lattice-like protrusions seen in epithelial cells. These T6SS-induced protrusion patterns are suggestive of normal Arp2/3 complex activity, which situates itself at 70° F-actin branch points and

organizes F-actin polymerization within a dendritic array at the periphery of lamellipodia (Koestler *et al.*, 2008). During infection, polymerization of actin may be functioning normally, but host macrophages may have lost the ability to retract their lamellipodia and pseudopodia, or otherwise depolymerize actin (Ponti *et al.*, 2004).

It has been shown that constitutive over-expression of Rac1 by host cells prevented disruption of cortical actin by *B. cenocepacia* and host cells assumed a normal morphology (Grinstein and Valvano, unpublished). Rac1 is involved in the normal regulation of pseudopod protrusion at the leading edge of migratory cells, and the presence of Rho antagonizes the development of protrusions (Ohta *et al.*, 2006; Burridge and Doughman, 2006). If either of these proteins is modulated by the T6SS, the result would be irregular protrusion from areas other than the leading edge of the cell. The protrusion phenotype may also be the consequence of insufficient retraction of actin, and focal adhesions unable to detach from the substrate while a macrophage migrates. In effect, the protrusion phenotype may result from pseudopods that cannot retract as the macrophage moves.

The actin cytoskeleton is also important for fusion events between the maturing phagosome and endosomal pathway (Kjeken *et al.*, 2004). Since intracellular *B. cenocepacia* can induce remodeling of the host cell actin cytoskeleton via its T6SS (Aubert *et al.*, 2008), we hypothesized that the T6SS could have a role in the phagosome maturation delay induced by *B. cenocepacia* (Lamothe *et al.*, 2007). Our results clearly demonstrate that the presence or absence of a functional T6SS does not alter the LAMP-1 recruitment to the bacteria-containing vacuole.

Even though the T6SS of *B. cenocepacia,* in particular, does not appear to alter the maturation pattern of the phagosome, the T6SS of other bacterial species has been linked to modification of that compartment. In the case of *Francisella tularensis*, the T6SS is required for the escape of the pathogen from maturing phagosomes into the cytosol where it then replicates and causes the induction of caspase-1 dependent cell death (Chong *et al.,* 2008). Although lysosome fusion requires the presence of LAMP-1 on the phagosomal membrane, this does not mean that fusion necessarily must occur due to the presence of the LAMP-1 protein. *Campylobacter jejuni* can survive in a LAMP-1 positive vacuole which has left the normal phagosomal maturation sequence, and which does not fuse with lysosomes (Watson and Galán, 2008). Therefore, follow-up studies utilizing a lysosome specific dye would determine if the T6SS mediates exceptional circumstances, such as LAMP-1 recruitment but lack of lysosome fusion similar to *C. jejuni.*

4.2. Role of the T6SS in the induction of macrophage cell death

This study was prompted by the observation that the T6SS expression of *B. cenocepacia* correlates with either loss-of-adherence or cell death of infected macrophages, as determined by a DAPI-based adherence assay developed during this project. Data generated using that assay was corroborated by a more specific analysis using flow cytometry. Indeed, significant reduction in host cell death mediated by *B. cenocepacia* was only observed in macrophages infected with strains that were T6SS-defective (through the deletion of *hcp*) in conjunction with loss of normal regulation (through the deletion or inactivation of *atsR*). Either mutation

alone did not result in decreased host cell death beyond levels found with the K56-2 wild-type strain.

Alternative explanations were addressed for why only the double-mutants, either K56-2 Δ*hcp atsR*::pDA27 or K56-2 Δ*hcp* Δ*atsR*, were compromised for the induction of host cell death. Excessive production of T6SS components, in the absence of *atsR*, without an intact secretion apparatus could cause reduced fitness of bacteria or a growth defect. This potential explanation was ruled out given there was no significant growth defect between parental K56-2 and mutant strains grown in LB broth. The K56-2 Δ*hcp* strain retained the T6SS-defective phenotype as it was not capable of inducing the actin-rich protrusions, but this strain was still capable of inducing cell death. This suggests that the protrusion phenotype does not necessarily play a role in cell death, and strongly indicates that the T6SS is not the sole virulence factor or secretion system responsible for host cell death by *B. cenocepacia*. Furthermore, it is unlikely that the observed phenotype is due to another gene being mutated as disruption of *atsR* cannot affect downstream genes via polar effects because *atsR* is the final gene of a three-gene operon (Aubert *et al.,* 2008).

Dual regulation by AtsR of both the T6SS and an unknown virulence factor may exist. The *atsR* gene of *B. cenocepacia* displays homology to the *retS* gene of *P. areuginosa,* and RetS is a key player in a complex regulatory cascade controlling the T6SS and biofilm formation (Goodman *et al.,* 2004; Laskowski and Kazmierczak, 2006). Though it has been shown that AtsR is a global negative regulator of the T6SS, it may also function as a positive regulator of at least one other unknown

virulence factor, or for other regulators. The cell death observed in host cells infected with K56-2 Δ*atsR* may be the consequence of a functional T6SS. During K56-2 Δ*hcp* infection, cell death may be the result of an alternate virulence factor or group of factors that is "unmasked" in the absence of a functional T6SS. When both genes are disrupted or deleted, as is the case with K56-2 Δ*hcp* Δ*atsR*, we may have a situation where no compensatory virulence factor exists for the non-functional T6SS, and as a result, the incidence of host cell death is significantly reduced. Given that cell death during K56-2 Δ*hcp* Δ*atsR* infection is not reduced to levels observed for uninfected macrophages, the situation may be more complex. Cheung *et al.* (2007) have demonstrated that the cable pilus of *B. cenocepacia* K56-2 is directly involved in causing host cell death, but loss of the *cblA* gene, which is required for production of the cable pilus, does not result in the recovery of host cell viability to uninfected levels (Cheung *et al.*, 2007). Incorporating experimentation with both *cblA* and T6SS mutations may be informative.

Another factor that may account for cell death during K56-2 Δ*hcp* Δ*atsR* infection could be the uncontrolled presence of extracellular bacteria. We were unable to eliminate the growth of extracellular *B. cenocepacia* due to the pathogen's extreme antibiotic resistance. Over the course of 24-hour infections during this study, media used during co-incubation of macrophages with *B. cenocepacia* became turbid with bacterial growth. Though the initial MOI was 10 bacteria per macrophage at time zero, by 24 hours post-infection, the MOI could be several folds higher. The K56-2 *mgtC*::pKM3 strain was used to control for the presence of extracellular bacteria, as it functions similarly to heat-killed K56-2 wild-type once

internalized by a macrophage, but is otherwise normal (Maloney & Valvano, 2006). However, results indicated that the K56-2 *mgtC*::pKM3 mutant is still capable of inducing both cell death and the T6SS-mediated protrusion phenotype, suggesting that both phenotypes may be induced early on during infection, before this mutant can be degraded during the normal maturation process of the phagosome. Another possibility is that the K56-2 *mgtC*::pKM3 mutant is capable of surviving within phagosomes despite previous observations (Maloney and Valvano, 2006). To address the problem of extracellular bacterial growth, our lab has recently produced a gentamicin-sensitive K56-2 mutant. This mutant, if proven to traffic through phagosome maturation identically to wild-type *B. cenocepacia*, may facilitate the study of cell death mechanisms without the influence of extracellular bacteria.

As mentioned, the initial inoculum of each K56-2 strain grew enough to cause broth turbidity within 24 hours when coincubated with macrophages under standard tissue culture growth conditions. However, none of the strains studied had a growth defect when grown in LB broth during a bioscreen experiment. This partially ruled out the possibility that the K56-2 Δ*hcp* Δ*atsR* strain was deficient in extracellular growth around macrophages, which would result in fewer phagocytized bacteria. To be confident that there was no growth defect between strains during macrophage infection, growth needed to be tested in DMEM. However, K56-2 strains did not grow during a bioscreen experiment when inoculated into DMEM and three derivatives. This suggested that extracellular growth during infection experiments resulted from bacteria scavenging nutrients from live macrophages, or utilizing nutrients obtained from dead macrophage

debris, or possibly replication within macrophages and escape to the extracellular media following cell death. Another explanation is a requirement for atmospheric carbon dioxide when the bacteria are grown in DMEM-based media. The presence of carbon dioxide is a key difference between the atmosphere of the bioscreen and that of tissue culture growth chambers. The mechanism of how *B. cenocepacia* may be facilitating its growth in the extracellular media through nutrient scavenging is unknown, but exploration of this point was beyond the scope of the current project.

To more specifically address the cell death phenotype during K56-2 infection of macrophages, a caspase-3-specific inhibitor of cell death, Ac-DMQD-CHO, was used in an attempt to rescue macrophages from bacteria-induced cell death, therefore, pinpointing a mechanism exploited by bacteria. Following 24-hour infection with K56-2 wild-type, no significant difference was noted between cells not pre-treated with the inhibitor and those cells treated with two different concentrations of Ac-DMQD-CHO. This suggests that caspase-3 may not be involved in cell death mediated by *B. cenocepacia*. These results are surprising considering the consistent annexin V-positive flow cytometry data that suggested apoptosis. However, one important control was lacking during this experiment. We were not capable of demonstrating that Ac-DMQD-CHO could rescue ANA-1 macrophages from actinomycin D-mediated apoptosis, even when actinomycin D was administered at concentrations of 50 ng/mL (data not shown). This suggests that the inhibitor was not effective at inhibiting caspase-3, or that this particular cell type was more sensitive to actinomycin D than other macrophage cell types used previously in the literature. Increased sensitivity to actinomycin D would require

greater concentrations of caspase-3 inhibitor to compensate. However, the concentration of Ac-DMQD-CHO could not safely be increased beyond 50 μM, as excessive concentrations of caspase inhibitors result in loss of caspase-specificity and increase cross-reaction with caspase enzymes that have similar pentapeptide substrates (Pereira and Song, 2008). In the case of the pan-caspase inhibitor, Z-VAD-FMK, concentrations of 100 μM have been shown to actually induce cell death, through Rip-1 kinase dependent pathways (Martinet *et al.,* 2006a; Martinet *et al.,* 2006b). For these reasons, concentrations higher than 50 μM were not likely to provide reliable results.

4.3 - A model for molecular pathogenesis induced by the T6SS of *B. cenocepacia*

This project studied downstream effects on the host cell following regulation of the T6SS by *B. cenocepacia*. These downstream effects include the remodeling of host cell actin, and T6SS involvement in the induction of host cell death. Though the T6SS was not directly involved in delaying recruitment of LAMP-1 to the BcCV membrane, based on data from this project we propose a model for an interaction of these three phenomena.

After phagocytosis, wild-type *B. cenocepacia* is found within a normally maturing phagosome. Through some unknown mechanism, *B. cenocepacia* delays this maturation process between a point after EEA-1 dissociation from the BcCV membrane but prior to the acquisition of LAMP-1 (Lamothe *et al.,* 2007). From this study we learned that BcCVs in ANA-1 macrophages first begin acquisition of LAMP-

1 between 6 and 8 hours post-infection. This extended time spent within a niche compartment may allow for sufficient T6SS expression by internalized bacteria to induce changes to the host cell cytoskeleton, or this time may allow for intraphagosomal replication, after which bacteria may collectively express the T6SS to levels adequate for the remodeling of the host cell actin cytoskeleton. In either case, the delay in phagosome maturation may be crucial for the actin cytoskeleton rearrangement. At approximately 6 hours post-infection, K56-2 wild-type induces the formation of actin-rich protrusions. At 10 hours post-infection, LAMP-1 is acquired by the majority of BcCVs, and as early as 12 hours post-infection, the induction of host cell death begins, through an unknown mechanism resembling apoptosis. This model suggests that as the BcCV becomes subverted by the host, the pathogen responds to losing its intracellular niche by upregulating its T6SS and unknown complementary virulence factors to induce actin rearrangements, and host cell death. This response may prolong the survival of intracellular bacteria, but may more generally arrest the function of phagocytic cells, enabling the uncontrolled growth of extracellular bacteria in the process. Recently, the notion of pathogen "martyrdom" mediated by T6SS to stop the functioning of phagocytic host cells has been introduced based on research in *V. cholerae* (Ma *et al.,* 2009; Satchell, 2009). If internalized *B. cenocepacia* bacteria are capable of preventing phagocytic cell migratory behaviour, inducing host cell death and escaping to the extracellular milieu, the resultant uncontrolled spread of infection could have severe consequences for the host.

4.4 - Future Directions

To more fully characterize cell death induced by *B. cenocepacia*, the role of AtsR in its regulatory network will need to be studied in greater depth. The reduction of cell death during K56-2 Δ*hcp* Δ*atsR* infection but not during K56-2 Δ*hcp* infection suggests that regulation by AtsR controls cell death-oriented virulence factors other than the T6SS alone. Therefore, identifying the complementary virulence factor(s) that may be involved is critical to the success of this study in the future, and understanding the AtsR regulatory network more fully may be the first step to finding complementary virulence factors to the T6SS.

An aspect of this study that could not be adequately addressed was the presence of extracellular bacteria. A gentamicin-sensitive K56-2 mutant will enable the study of cell death without the growth of extracellular bacteria, and may elucidate whether *B. cenocepacia* replicates intracellularly as a prelude to that cell death. The use of this strain will, therefore, form the backbone of most future experiments with K56-2 infection of macrophages, including determining if intracellular growth occurs prior to some form of host cytolysis, similar to *L. pneumophila.*

From a host cell perspective, actin regulatory proteins that could be candidate targets for modulation should be investigated. Small GTPases are known targets of other intracellular pathogens, and in the case of *B. cenocepacia,* Rac1 and Rho may be promising candidates. Rac1 may not only be involved in the development of the protrusion phenotype, as it is also a component of the NADPH oxidase complex, which undergoes a delayed assembly process during infection

with *B. cenocepacia* (Keith *et al.,* 2009). Rac1 and its antagonists may be a useful candidates to study for the characterization of actin remodeling mediated by *B. cenocepacia.*

4.5 - Conclusion

This project has looked broadly at several aspects of *B. cenocepacia* pathogenesis facilitated by the T6SS. This secretion system has only recently been discovered and its characterization is still in its infancy. Thus far, in all but a few rare cases, the T6SS is consistently linked to pathogenesis. It is possible that the pathogen uses its T6SS to contribute to its persistence in the host. This is supported by previous evidence in our laboratory showing that T6SS defective mutants are highly attenuated in the rat animal model of chronic lung infection (Hunt *et al.,* 2004). Continued study in our lab will help determine if this is the case, and if so, how best to develop targeted therapeutic agents against *B. cenocepacia.*

Literature Cited

Abeliovich, D., Lavon, I. P., Lerer, I., Cohen, T., Springer, C., Avital, A. & Cutting, G. R. (1992). Screening for five mutations detects 97% of cystic fibrosis (CF) chromosomes and predicts a carrier frequency of 1:29 in the Jewish Ashkenazi population. *Am J Hum Genet* 51, 951-956.

Abraham, M. C. & Shaham, S. (2004). Death without caspases, caspases without death. *Trends Cell Biol* 14, 184-193.

Aubert, D. F., Flannagan, R. S. & Valvano, M. (2008). A novel sensor kinase-response regulator hybrid controls biofilm formation and type VI secretion system activity in *Burkholderia cenocepacia. Infection and Immunity* 76, 1979-1991.

Ballard, R. W., Palleroni, N. J., Doudoroff, M., Stanier, R. Y. & Mandel, M. (1970). Taxonomy of the aerobic pseudomonads: *Pseudomonas cepacia, P. marginata, P. alliicola* and *P. caryophylli. J Gen Microbiol* 60, 199-214.

Ballister, E. R., Lai, A. H., Zuckermann, R. N., Cheng, Y. & Mougous, J. (2008). In vitro self-assembly of tailorable nanotubes from a simple protein building block. *Proc Natl Acad Sci USA* 105, 3733-3738.

Bandyopadhyay, P., Xiao, H., Coleman, H. A., Price-Whelan, A. & Steinman, H. M. (2004). Icm/dot-independent entry of *Legionella pneumophila* into amoeba and macrophage hosts. *Infection and Immunity* 72, 4541-4551.

Bardill, J. P., Miller, J. L. & Vogel, J. P. (2005). IcmS-dependent translocation of SdeA into macrophages by the *Legionella pneumophila* type IV secretion system. *Molecular Microbiology* 56, 90-103.

Bevivino, A., Tabacchioni, S., Chiarini, L., Carusi, M. V., Del Gallo, M. & Visca, P. (1994). Phenotypic comparison between rhizosphere and clinical isolates of *Burkholderia cepacia. Microbiology* 140, 1069-1077.

Bingle, L. E., Bailey, C. M. & Pallen, M. J. (2008). Type VI secretion: a beginner's guide. *Curr Opin Microbiol* 11, 3-8.

Blocker, A., Jouihri, N., Larquet, E., Gounon, P., Ebel, F., Parsot, C., Sansonetti, P. & Allaoui, A. (2001). Structure and composition of the *Shigella flexneri* "needle complex", a part of its type III secreton. *Molecular Microbiology* 39, 652-663.

Bönemann, G., Pietrosiuk, A., Diemand, A., Zentgraf, H. & Mogk, A. (2009). Remodelling of VipA/VipB tubules by ClpV-mediated threading is crucial for type VI protein secretion. *EMBO J* 28, 315-325.

Bottone, E. J., Douglas, S. D., Rausen, A. R. & Keusch, G. T. (1975). Association of *Pseudomonas cepacia* with chronic granulomatous disease. *J Clin Microbiol* 1, 425-428.

Burkholder, W. H. (1950). Sour skin, a bacterial rot of onion bulbs. *Phytopathol* 40, 115-117.

Burridge, K. & Doughman, R. (2006). Front and back by Rho and Rac. *Nat Cell Biol* 8, 781-782.

Cain, R., Hayward, R. & Koronakis, V. (2004). The target cell plasma membrane is a critical interface for *Salmonella* cell entry effector-host interplay. *Molecular Microbiology* 54, 887-904.

Cascales, E. (2008). The type VI secretion toolkit. *EMBO Rep* 9, 735-741.

Cheng, S. H., Gregory, R. J., Marshall, J., Paul, S., Souza, D. W., White, G. A., O'Riordan, C. R. & Smith, A. E. (1990). Defective intracellular transport and processing of CFTR is the molecular basis of most cystic fibrosis. *Cell* 63, 827-834.

Cheung, K. J., Li, G., Urban, T., Goldberg, J., Griffith, A., Lu, F. & Burns, J. L. (2007). Pilus-mediated epithelial cell death in response to infection with *Burkholderia cenocepacia*. *Microbes Infect* 9, 829-837.

Chong, A., Wehrly, T. D., Nair, V., Fischer, E. R., Barker, J. R., Klose, K. E. & Celli, J. (2008). The early phagosomal stage of *Francisella tularensis* determines optimal phagosomal escape and *Francisella* pathogenicity island protein expression. *Infection and Immunity* 76, 5488-5499.

Cicchetti, G., Maurer, P., Wagener, P. & Kocks, C. (1999). Actin and phosphoinositide binding by the ActA protein of the bacterial pathogen *Listeria monocytogenes*. *Journal of Biological Chemistry*.

Coenye, T. & Vandamme, P. (2003). Diversity and significance of *Burkholderia* species occupying diverse ecological niches. *Environ Microbiol* 5, 719-729.

Cornelis, G. (2006). The type III secretion injectisome. *Nat Rev Micro* 4, 811-825.

Cox, D., Tseng, C. C., Bjekic, G. & Greenberg, S. (1999). A requirement for phosphatidylinositol 3-kinase in pseudopod extension. *J Biol Chem* 274, 1240-1247.

Daleke, D. L. (2003). Regulation of transbilayer plasma membrane phospholipid asymmetry. *J Lipid Res* 44, 233-242.

Das, S. & Chaudhuri, K. (2003). Identification of a unique IAHP (IcmF associated homologous proteins) cluster in *Vibrio cholerae* and other proteobacteria through in silico analysis. *In Silico Biol* 3, 287-300.

Degterev, A. & Yuan, J. (2008). Expansion and evolution of cell death programmes. *Nat Rev Mol Cell Biol* 9, 378-390.

Delepelaire, P. (2004). Type I secretion in gram-negative bacteria. *Biochim Biophys Acta* 1694, 149-161.

Desjardins, M., Huber, L. A., Parton, R. G. & Griffiths, G. (1994). Biogenesis of phagolysosomes proceeds through a sequential series of interactions with the endocytic apparatus. *J Cell Biol* 124, 677-688.

Dos Remedios, C. G., Chhabra, D., Kekic, M. & Dedova, I. V. (2003). Actin binding proteins: regulation of cytoskeletal microfilaments. *Physio Rev* 83, 433-473.

Dupuis, A., Hamilton, D., Cole, D. E. & Corey, M. (2005). Cystic fibrosis birth rates in Canada: a decreasing trend since the onset of genetic testing. *J Pediatr* 147, 312-315.

Ellis, H. M. & Horvitz, H. R. (1986). Genetic control of programmed cell death in the nematode C. elegans. *Cell* 44, 817-829.

Estrada-De Los Santos, P., Bustillos-Cristales, R. & Caballero-Mellado, J. (2001). *Burkholderia*, a genus rich in plant-associated nitrogen fixers with wide environmental and geographic distribution. *Appl Environ Microbiol* 67, 2790-2798.

Fink, S. L. & Cookson, B. T. (2005). Apoptosis, pyroptosis, and necrosis: mechanistic description of dead and dying eukaryotic cells. *Infection and Immunity* 73, 1907-1916.

Gao, L. Y. & Abu Kwaik, Y. (1999). Activation of caspase 3 during *Legionella pneumophila*-induced apoptosis. *Infection and Immunity* 67, 4886-4894.

Gentschev, I., Dietrich, G. & Goebel, W. (2002). The E. coli alpha-hemolysin secretion system and its use in vaccine development. *Trends Microbiol* 10, 39-45.

Gerlach, R. G. & Hensel, M. (2007). Protein secretion systems and adhesins: the molecular armory of Gram-negative pathogens. *Int J Med Microbiol* 297, 401-415.

Goodman, A. L., Kulasekara, B., Rietsch, A., Boyd, D., Smith, R. S. & Lory, S. (2004). A signaling network reciprocally regulates genes associated with acute infection and chronic persistence in *Pseudomonas aeruginosa*. *Dev Cell* 7, 745-754.

Heyworth, P. G., Cross, A. R. & Curnutte, J. T. (2003). Chronic granulomatous disease. *Current Opinion in Immunology* 15, 578-584.

Holland, S. M. (2009). Chronic Granulomatous Disease. *Clin Reviews Allerg Immunol* (electronic publication ahead of print).

Horwitz, M. A. (1983). Formation of a novel phagosome by the Legionnaires' disease bacterium (*Legionella pneumophila*) in human monocytes. *J Exp Med* 158, 1319-1331.

Hunt, T. A., Kooi, C., Sokol, P. A. & Valvano, M. (2004). Identification of *Burkholderia cenocepacia* genes required for bacterial survival in vivo. *Infection and Immunity* 72, 4010-4022.

Huynh, K., Eskelinen, E., Scott, C., Malevanets, A., Saftig, P. & Grinstein, S. (2007). LAMP proteins are required for fusion of lysosomes with phagosomes. *EMBO J* 26, 313-324.

Jin, Q. & He, S. Y. (2001). Role of the Hrp pilus in type III protein secretion in Pseudomonas *syringae*. *Science* 294, 2556-2558.

Keith, K. E., Hynes, D. W., Sholdice, J. E. & Valvano, M. (2009). Delayed association of the NADPH oxidase complex with macrophage vacuoles containing the opportunistic pathogen *Burkholderia cenocepacia*. *Microbiology* 155, 1004-1015.

Kirby, J. E., Vogel, J. P., Andrews, H. L. & Isberg, R. R. (1998). Evidence for pore-forming ability by *Legionella pneumophila*. *Molecular Microbiology* 27, 323-336.

Kjeken, R., Egeberg, M., Habermann, A. & other authors (2004). Fusion between phagosomes, early and late endosomes: a role for actin in fusion between late, but not early endocytic organelles. *Mol Biol Cell* 15, 345-358.

Koestler, S. A., Auinger, S., Vinzenz, M., Rottner, K. & Small, J. V. (2008). Differentially oriented populations of actin filaments generated in lamellipodia collaborate in pushing and pausing at the cell front. *Nat Cell Biol* 10, 306-313.

Koronakis, V., Sharff, A., Koronakis, E., Luisi, B. & Hughes, C. (2000). Crystal structure of the bacterial membrane protein TolC central to multidrug efflux and protein export. *Nature* 405, 914-919.

Kwaik, Y. A. (1998). Fatal attraction of mammalian cells to *Legionella pneumophila*. *Molecular Microbiology* 30, 689-695.

Lakeman, P., Gille, J. J., Dankert-Roelse, J. E. & other authors (2008). CFTR mutations in Turkish and North African cystic fibrosis patients in Europe: implications for screening. *Genet Test* 12, 25-35.

Lamothe, J., Huynh, K., Grinstein, S. & Valvano, M. (2007). Intracellular survival of *Burkholderia cenocepacia* in macrophages is associated with a delay in the maturation of bacteria-containing vacuoles. *Cellular Microbiology* 9, 40-53.

Lamothe, J. & Valvano, M. (2008). *Burkholderia cenocepacia*-induced delay of acidification and phagolysosomal fusion in cystic fibrosis transmembrane conductance regulator (CFTR)-defective macrophages. *Microbiology* 154, 3825-3834.

Laskowski, M. A. & Kazmierczak, B. I. (2006). Mutational analysis of RetS, an unusual sensor kinase-response regulator hybrid required for *Pseudomonas aeruginosa* virulence. *Infection and Immunity* 74, 4462-4473.

Leiman, P. G., Basler, M., Ramagopal, U. A., Bonanno, J. B., Sauder, J. M., Pukatzki, S., Burley, S. K., Almo, S. C. & Mekalanos, J. (2009). Type VI secretion apparatus and phage tail-associated protein complexes share a common evolutionary origin. *Proc Natl Acad Sci USA* 106, 4154-4159.

Lukacs, G. L., Rotstein, O. D. & Grinstein, S. (1990). Phagosomal acidification is mediated by a vacuolar-type H(+)-ATPase in murine macrophages. *J Biol Chem* 265, 21099-21107.

Ma, A. T., Mcauley, S., Pukatzki, S. & Mekalanos, J. (2009). Translocation of a *Vibrio cholerae* type VI secretion effector requires bacterial endocytosis by host cells. *Cell Host Microbe* 5, 234-243.

Mahenthiralingam, E., Baldwin, A. & Dowson, C. G. (2008). *Burkholderia cepacia* complex bacteria: opportunistic pathogens with important natural biology. *J Appl Microbiol* 104, 1539-1551.

Mahenthiralingam, E., Baldwin, A., Drevinek, P., Vanlaere, E., Vandamme, P., Lipuma, J. & Dowson, C. G. (2006). Multilocus sequence typing breathes life into a microbial metagenome. *PLoS ONE* 1, e17.

Mahenthiralingam, E., Urban, T. & Goldberg, J. (2005). The multifarious, multireplicon *Burkholderia cepacia* complex. *Nat Rev Micro* 3, 144-156.

Malaisse, W. J., Svoboda, M., Dufrane, S. P., Malaisse-Lagae, F. & Christophe, J. (1984). Effect of *Bordetella pertussis* toxin on ADP-ribosylation of membrane proteins, adenylate cyclase activity and insulin release in rat pancreatic islets. *Biochemical and Biophysical Research Communications* 124, 190-196.

Maloney, K. E. & Valvano, M. (2006). The mgtC gene of *Burkholderia cenocepacia* is required for growth under magnesium limitation conditions and intracellular survival in macrophages. *Infection and Immunity* 74, 5477-5486.

Mars, A. E., Houwing, J., Dolfing, J. & Janssen, D. B. (1996). Degradation of Toluene and Trichloroethylene by *Burkholderia cepacia* G4 in Growth-Limited Fed-Batch Culture. *Appl Environ Microbiol* 62, 886-891.

Marshall, J. G., Booth, J. W., Stambolic, V., Mak, T., Balla, T., Schreiber, A. D., Meyer, T. & Grinstein, S. (2001). Restricted accumulation of phosphatidylinositol 3-kinase products in a plasmalemmal subdomain during Fc gamma receptor-mediated phagocytosis. *J Cell Biol* 153, 1369-1380.

Martinet, W., De Meyer, G. R., Timmermans, J. P., Herman, A. G. & Kockx, M. M. (2006). Macrophages but not smooth muscle cells undergo benzyloxycarbonyl-Val-Ala-DL-Asp(O-Methyl)-fluoromethylketone-induced nonapoptotic cell death depending on receptor-interacting protein 1 expression: implications for the stabilization of macrophage-rich atherosclerotic plaques. *J Pharmacol Exp Ther* 317, 1356-1364.

Martinet, W., Schrijvers, D. M., Herman, A. G. & De Meyer, G. R. (2006). z-VAD-fmk-induced non-apoptotic cell death of macrophages: possibilities and limitations for atherosclerotic plaque stabilization. *Autophagy* 2, 312-314.

Minakami, R. & Sumimotoa, H. (2006). Phagocytosis-coupled activation of the superoxide-producing phagocyte oxidase, a member of the NADPH oxidase (nox) family. *Int J Hematol* 84, 193-198.

Mougous, J., Cuff, M. E., Raunser, S. & other authors (2006). A virulence locus of *Pseudomonas aeruginosa* encodes a protein secretion apparatus. *Science* 312, 1526-1530.

Mougous, J., Gifford, C., Ramsdell, T. & Mekalanos, J. (2007). Threonine phosphorylation post-translationally regulates protein secretion in *Pseudomonas aeruginosa*. *Nat Cell Biol* 9, 797-803.

Nunn, D. N. & Lory, S. (1993). Cleavage, methylation, and localization of the *Pseudomonas aeruginosa* export proteins XcpT, -U, -V, and -W. *J Bacteriol* 175, 4375-4382.

O'Sullivan, B. P. & Freedman, S. D. (2009). Cystic fibrosis. *Lancet* 373, 1891-1904.

Ohta, Y., Hartwig, J. H. & Stossel, T. P. (2006). FilGAP, a Rho- and ROCK-regulated GAP for Rac binds filamin A to control actin remodelling. *Nat Cell Biol* 8, 803-814.

Pell, L. G., Kanelis, V., Donaldson, L. W., Howell, P. L. & Davidson, A. R. (2009). The phage lambda major tail protein structure reveals a common evolution for long-tailed phages and the type VI bacterial secretion system. *Proc Natl Acad Sci USA* 106, 4160-4165.

Pereira, N. A. & Song, Z. (2008). Some commonly used caspase substrates and inhibitors lack the specificity required to monitor individual caspase activity. *Biochem Biophys Res Commun* 377, 873-877.

Pohlner, J., Halter, R., Beyreuther, K. & Meyer, T. F. (1987). Gene structure and extracellular secretion of *Neisseria gonorrhaeae* IgA protease. *Nature* 325, 458-462.

Ponti, A., Machacek, M., Gupton, S. L., Waterman-Storer, C. M. & Danuser, G. (2004). Two distinct actin networks drive the protrusion of migrating cells. *Science* 305, 1782-1786.

Porter, A. G. & Jänicke, R. U. (1999). Emerging roles of caspase-3 in apoptosis. *Cell Death Differ* 6, 99-104.

Pugsley, A. P., Francetic, O., Hardie, K., Possot, O. M., Sauvonnet, N. & Seydel, A. (1997). Pullulanase: model protein substrate for the general secretory pathway of gram-negative bacteria. *Folia Microbiol* 42, 184-192.

Pukatzki, S., Ma, A. T., Revel, A. T., Sturtevant, D. & Mekalanos, J. (2007). Type VI secretion system translocates a phage tail spike-like protein into target cells where it cross-links actin. *Proc Natl Acad Sci USA* 104, 15508-15513.

Pukatzki, S., Ma, A. T., Sturtevant, D., Krastins, B., Sarracino, D., Nelson, W. C., Heidelberg, J. F. & Mekalanos, J. (2006). Identification of a conserved bacterial protein secretion system in *Vibrio cholerae* using the *Dictyostelium* host model system. *Proc Natl Acad Sci USA* 103, 1528-1533.

Quitard, S., Dean, P., Maresca, M. & Kenny, B. (2006). The enteropathogenic *Escherichia coli* EspF effector molecule inhibits PI-3 kinase-mediated uptake independently of mitochondrial targeting. *Cellular Microbiology* 8, 972-981.

Sajjan, U., Yang, J., Hershenson, M. & Lipuma, J. (2006). Intracellular trafficking and replication of *Burkholderia cenocepacia* in human cystic fibrosis airway epithelial cells. *Cellular Microbiology* 8, 1456-1466.

Sandkvist, M. (2001). Biology of type II secretion. *Mol Micro* 40, 271-283.

Sandkvist, M., Bagdasarian, M., Howard, S. P. & DiRita, V. J. (1995). Interaction between the autokinase EpsE and EpsL in the cytoplasmic membrane is required for extracellular secretion in *Vibrio cholerae*. *EMBO J* 14, 1664-1673.

Satchell, K. J. (2009). Bacterial martyrdom: phagocytes disabled by type VI secretion after engulfing bacteria. *Cell Host Microbe* 5, 213-214.

Schlieker, C., Zentgraf, H., Dersch, P. & Mogk, A. (2005). ClpV, a unique Hsp100/Clp member of pathogenic proteobacteria. *Biol Chem* 386, 1115-1127.

Schmidt, H. & Hensel, M. (2004). Pathogenicity islands in bacterial pathogenesis. *Clin Microbiol Rev* 17, 14-56.

Schülein, R., Gentschev, I., Mollenkopf, H. J. & Goebel, W. (1992). A topological model for the haemolysin translocator protein HlyD. *Mol Gen Genet* 234, 155-163.

Scorrano, L. & Korsmeyer, S. J. (2003). Mechanisms of cytochrome c release by proapoptotic BCL-2 family members. *Biochem Biophys Res Commun* 304, 437-444.

Speert, D., Henry, D., Vandamme, P., Corey, M. & Mahenthiralingam, E. (2002). Epidemiology of *Burkholderia cepacia* complex in patients with cystic fibrosis, Canada. *Emerging Infect Dis* 8, 181-187.

Spilker, T., Baldwin, A., Bumford, A., Dowson, C. G., Mahenthiralingam, E. & Lipuma, J. J. (2009). Expanded Multilocus Sequence Typing for *Burkholderia* Species. *J Clin Microbiol.*

Thornberry, N. A. & Lazebnik, Y. (1998). Caspases: enemies within. *Science* 281, 1312-1316.

Valvano, M., Keith, K. E. & Cardona, S. T. (2005). Survival and persistence of opportunistic *Burkholderia* species in host cells. *Curr Opin Microbiol* 8, 99-105.

van Bueren, A. L., Higgins, M., Wang, D., Burke, R. D. & Boraston, A. B. (2007). Identification and structural basis of binding to host lung glycogen by streptococcal virulence factors. *Nat Struct Mol Biol* 14, 76-84.

Vandamme, P., Holmes, B., Coenye, T., Goris, J., Mahenthiralingam, E., Lipuma, J. & Govan, J. R. (2003). *Burkholderia cenocepacia* sp. nov.--a new twist to an old story. *Res Microbiol* 154, 91-96.

Vandamme, P., Holmes, B., Vancanneyt, M. & other authors (1997). Occurrence of multiple genomovars of *Burkholderia cepacia* in cystic fibrosis patients and proposal of *Burkholderia multivorans* sp. nov. *Int J Syst Bacteriol* 47, 1188-1200.

Vandamme, P. & Mahenthiralingam, E. (2003). Strains from the *Burkholderia cepacia* Complex: Relationship to Opportunistic Pathogens. *J Nematol* 35, 208-211.

Vandamme, P., Pot, B., Gillis, M., de Vos, P., Kersters, K. & Swings, J. (1996). Polyphasic taxonomy, a consensus approach to bacterial systematics. *Microbiol Rev* 60, 407-438.

Vieira, O. V., Botelho, R. J. & Grinstein, S. (2002). Phagosome maturation: aging gracefully. *Biochem J* 366, 689-704.

Waldor, M. K., Tschäpe, H. & Mekalanos, J. J. (1996). A new type of conjugative transposon encodes resistance to sulfamethoxazole, trimethoprim, and streptomycin in *Vibrio cholerae* O139. *J Bacteriol* 178, 4157-4165.

Wandersman, C., Delepelaire, P., Letoffe, S. & Schwartz, M. (1987). Characterization of *Erwinia chrysanthemi* extracellular proteases: cloning and expression of the protease genes in *Escherichia coli*. *J Bacteriol* 169, 5046-5053.

Watson, R. O. & Galán, J. E. (2008). *Campylobacter jejuni* survives within epithelial cells by avoiding delivery to lysosomes. *PLoS Pathog* 4, e14.

Zielenski, J. (2000). Genotype and phenotype in cystic fibrosis. *Respiration* 67, 117-133.